UNICA UNIVERSITÀ DEGLI STUDI DI CAGLIARI

This is the Author's [*accepted*] manuscript version of the following contribution: (author name, title, publisher, ecc)

CORONEO VALENTINA

PROGRESS IN ORGANIC COATINGS

Colloidal silver as innovative multifunctional pigment: The effect of Ag concentration on the durability and biocidal activity of wood paints

The publisher's version is available at:

(cod. DOI: ...)*https://dx.doi.org/10.1016/j.porgcoat.2022.107354*

Colloidal silver as innovative multifunctional pigment: the effect of Ag concentration on the durability and biocidal activity of wood paints

Massimo Calovi[1]*, Valentina Coroneo[2], Sabrina Palanti[3], Stefano Rossi[1]

[1]Department of Industrial Engineering, University of Trento, Via Sommarive 9, 38123 Trento Italy;

[2] Department of Medical Sciences and Public Health, University of Cagliari, SS 554 Monserrato, 09042 Cagliari, Italy;

[3]Italian National Research Council Institute for Bio-Economy (CNR-IBE), 50019 Sesto Fiorentino, Italy.

*Corresponding author: massimo.calovi@unitn.it Tel.: +39-0461-282403

Abstract

This study aims to assess the effect of two different colloidal silver amount on the durability and biocidal activity of a water-borne wood paint. The influence of this multifunctional pigment on the aesthetical features of the coatings was evaluated by colorimetric measurements and optical microscopy observations. The durability of the samples was investigated by means of different accelerated degradation tests, such as the exposure in a climatic chamber and to UV-B radiations. Scanning electron microscope observations, infrared spectroscopy analysis and colorimetric inspections were carried out to highlight the residual influence of silver in altering the protective behavior of the paint. Moreover, the Ag-containing samples exhibited excellent antibacterial activity against *Staphylococcus aureus* and *Escherichia coli*, while colloidal silver did not introduce effective fungicidal performances against *Coniophora puteana* and *Trametes versicolor* fungi. Ultimately, this work demonstrates how colloidal silver can be used as a functional pigment in wood paint, capable of modifying the appearance of the coating, improving its antibacterial performance, without negatively affecting its protective performance.

Keywords: colloidal silver; wood paint; antimicrobial surfaces; public health; coatings durability.

1. Introduction

The wood industry represents a field of great importance and with enormous potential [1], as wood-based products are employed in various applications, such as construction [2], building [3, 4], furniture industry and interior decoration [5, 6]. As a matter of fact, the wood, in addition to particular aesthetic features, possesses several interesting characteristics, such as high strength-to-weight ratio [7], easy processing [8], and carbon neutral [9]. Nevertheless, the use of wood in various fields has often been restricted due to inherent limitations of the wood itself, such as its high flammability [10, 11] or poor durability when exposed to humidity [12, 13] and solar radiation [14-16].

To overcome these shortcomings of wood, the components are often coated with paints and organic layers [17-22], evaluating the coatings durability for interior [23] and outdoor [24] applications. The main task of the coating is to extend the service life of the component, safeguarding the wood from UV radiation [25], changes in humidity [26], chemical or mechanical attacks [27, 28], or from the detrimental presence of harmful organisms such as fungi [29, 30]. However, coatings are also often applied to provide the wood with particular aesthetic effects, through pronounced changes in color and gloss [31].

Recently, due to an extensive use of wood, many studies have focused on the use of nanofillers to further improve different performance of wood coatings [32]. For example, the UV absorption characteristics of wood coatings have been improved through incorporation of different nanoparticles. The solar light first decomposes lignin into radicals, which consequently provoke decomposition of other polymeric components, as hemicellulose and cellulose in the wood [21]. This phenomenon is highlighted by a clear discoloration of the wood [33, 34]. TiO_2 [35-37], ZnO [38, 39], SiO_2 [37, 40] and CeO_2 [41, 42] are commonly employed as nanofiller into organic coatings to protect the wood substrate from the UV radiations. Differently, the hardness, stiffness, and thermal stability of different nanostructures, such as nanosilica [43-45], nanoalumina [46, 47], nanoclay [48, 49] and nanocellulose [28, 50, 51], are usually exploited to refine the mechanical characteristics and water absorption of wood coatings [52].

However, one of the most significant aspects in terms of the improvement of the wood coatings deals with the prevention of the growth of microorganisms. Specifically, many works have focused on the study of the protection of wood coatings against bacteria [53-55] and fungi [56-58].

The proliferation of bacteria is a very topical issue, as the SARS-Cov-2 pandemic has shown. In fact, it has highlighted the need to find a solution to surface microbial contamination not only by focusing on highly critical environments (hospitals, nursing homes, etc.) but also in public spaces. This is true especially when conditions of high turnout occur, such as means of transport, gyms, supermarkets, airports, or schools. In these cases, it is crucial to recognize that transmission through contaminated surfaces is an important route for their diffusion [59, 60].

The constant disinfection of all touch-on surfaces [61] is not sustainable, in terms of relevant economic and temporal efforts, while its effectiveness is strongly dependent on the degree of

involvement of users [62]. As a result, the scientific community has tried to find alternative solutions to the typical disinfection procedures. The most practical way, which provides the best guarantees, is represented by the production of surfaces that intrinsically possess antimicrobial features [63-65], capable of killing or repelling the bacteria [66]. Inevitably, this approach involves also the wood-based products, due to their widespread use in public spaces [67, 68]. Wood coatings can offer antibacterial performance by incorporating nanomaterials such as copper nanopowders [69], nanocellulose [70] and nanotitanium [55, 71]. However, silver is the most effective antibacterial agent [72], as it offers the best biocidal characteristics, even in limited concentrations [73, 74]. The Ag ions, which are responsible for the antimicrobial activity, bond with the sulfhydryl groups of the proteins of the bacterial cell wall. By doing so, they modify their permeability, thus deactivating respiratory enzymes and hindering DNA replication [75]. However, the silver ions release is accompanied by other possible different action mechanisms [75, 76]. Some years ago, the antimicrobial efficacy of silver nanoparticles in transparent wood coatings for outdoor application has been assessed by 2 years of natural weathering [77]. However, the antibacterial performances of silver in organic coatings for wood applications have been confirmed by recent works [70, 78, 79], employing different silver forms [80].

Similarly, silver can also be used to improve the resistance to fungi of wood coatings [81]. Wood decay fungi represent one of the major elements of deterioration for wood, as they strongly reduce the durability of wood-based structures, acting both on non-enzymatic and enzymatic systems [82]. The presence of fungi can be deleterious even when the wood has been properly coated [83, 84]. Therefore, some works have attempted to improve the protection against fungal degradation of wood coatings, employing modified vegetable oils [85], copper [86] or combining fungicidal products such as propiconazole and thiabendazole [87]. Recently, several waterborne paints [88-90] exhibited an improvement of their resistance to fungi, thanks to the addition of silver nanoparticles [91, 92], confirming the good fungicidal activity of silver.

However, most of the studies on the antibacterial and fungicidal performances of wood coatings with silver additives do not concern about the effect introduced by silver itself, in terms of durability of the composite layer and changes of its aesthetic features. In fact, silver can introduce discontinuities in the organic matrix, favouring the penetration of aggressive substances for the wooden substrate and reducing the protective capability of the coating. At the same time, wood is also particularly appreciated for its unique appearance [23]: in fact, the vast majority of wood paints are transparent, pigment-free, to keep visible the natural appearance of the wood substrate. Nevertheless, the introduction of fillers in clear coatings could change its aesthetics. Thus, the purpose of this work is to evaluate the effect of colloidal silver on the durability and the aesthetic features of a waterborne paint for wood, studying its antibacterial and fungicidal performances. Two different amounts of colloidal silver were added to a commercial paint, to assess how the silver concentration influences the different coatings features.

The morphology and the aspect of the coatings were characterized by means of optical stereomicroscope, evaluating the effects introduced by the silver additive. The durability of the coatings was assessed subjecting the samples to accelerated degradation tests, such as the exposure in a climatic chamber and to UV-B radiations. The possible degradation of the coating caused by silver in the climatic chamber was evaluated by means of visual inspections and observations with the scanning electron microscope (SEM), while the adhesion of the coating was studied by means of the Cross Cut Test. On the other hand, FTIR analyses were used to monitor the chemical evolution of the coatings due to UV-B radiation exposures, evaluating the changes in aesthetic features by means of colorimetric investigations. Moreover, the antibacterial activity of the Ag-containing paints against *Staphylococcus aureus* and *Escherichia coli* were assessed as representatives of Gram-positive and Gram-negative bacteria, respectively. Finally, the fungicidal performances of the samples were characterized exposing the coatings to fungal attack of *Coniophora puteana* and *Trametes versicolor*.

2. Materials and methods

2.1 Materials

The colloidal silver (65–75 wt.% Ag) was purchased from Sigma-Aldrich (St. Louis, MO, USA) and used as received. The 50 × 50 × 2 mm^3 poplar wood substrates were supplied by OBI GmbH & Co (Wermelskirchen, Germany). The transparent water-borne paint WTVE097E30 was provided by ICRO Coatings S.p.A. (Bergamo, Italy). Polyurethane, dipropylen glycol monomethyl ether, paraffin and hydrocarbon waxes, dipropylenglicol n-butyl ether and 2-butoxyethanol are the most abundant components of this coating. However, the paint is considered a water-based product, as it does not contain organic solvents, but it shows a water concentration ≥ 75%. It possesses a dry residue equal to 34%, and a specific weight of 1.05 g/cm^3. The white acrylic-based primer Unimarc Smalto Seta was provided by San Marco Group (Venice, Italy) and used as received. The 40 x 70 x 2 mm^3 carbon steel substrate (Q-panel type R (0.15 wt.% C-Fe bal.) was supplied by Q-lab (Westlake, OH, USA). Nutrient Broth (NB), Nutrient Agar (NA), Plate Counting Agar (PCA), Phosphate Buffered Saline (1x PBS), purchased from Microbiol S.n.c. (Uta, Cagliari, Italy) were used for bacterial cultures and antibacterial tests, in accordance with BS ISO 22196: 2011 [93]. PBS was used for serial dilutions and to recover the bacterial cells from test samples. *Staphylococcus aureus* ATCC 6538 and *Escherichia coli* ATCC 25922 were purchased respectively from TCS Biosciences and Microbiologist (Bruker) operating in accordance with ISO 17034 for reference material producer. Fungal strains *C. puteana* Ebw 15 and *T. versicolor* CTB 863 were purchased from DMSZ, Germany. The cultura media for fungal growth was 40% malt and 20% agar from Scharlab srl (Lambro, Italy).

2.2 Samples production

The wood samples were first grinded using 320 grit sandpaper, to get a smooth surface. Subsequently, the water-borne paint provided by ICRO was sprayed onto the pre-treated wooden

surfaces, and the coatings were allowed to air dry at room temperature for 5 hours. The above process was repeated two times. However, the paint employed for the second application was modified by adding colloidal silver. Thus, the coatings were composed of two different layers. The first layer, without the presence of silver, was applied to guarantee protection to the wooden substrate, while the second one, the most external, possessed the Ag filler, in order to provide antimicrobial and antifungal properties to the coating. The colloidal silver granules were first dispersed in water, stirring the suspension for 30 min with an ultrasound probe, to facilitate the homogeneous distribution of the colloidal silver particles. Accordingly, the paint was diluted to 90% with the as-prepared silver-based suspension. Two different amounts of colloidal silver were employed in the formulation of the silver-based aqueous suspensions, to get a final concentration of Ag in the paint equal to 0.1 wt.% and 0.5 wt.%. In the two cases, to obtain 100 g of final product, 0.1 g and 0.5 g of colloidal silver were dispersed in 10 ml of water, respectively. Thus, the 10 ml of colloidal silver suspension was mixed with 90 g of paint. The performances of the two series of polyurethane-Ag coatings were compared with the behavior of a pure polyurethane layer, free of filler. The three samples series are summarized in **Table 1** with the samples nomenclature.

Samples Nomenclature	**Colloidal Silver Concentration (wt.%)**	
	First layer	**Second layer**
Ag0	0.0	0.0
Ag01	0.0	0.1
Ag05	0.0	0.5

Table 1: samples nomenclature.

2.3 Characterization

2.3.1 Coatings morphology and durability

Low vacuum scanning electron microscope SEM JEOL IT 300 (JEOL, Akishima, Tokyo, Japan) was used for the observation of the colloidal silver granules. The optical stereomicroscope Nikon SMZ25 (Nikon Instruments, Amstelveen, the Netherlands) was employed to analyze the surface morphology and the cross section of the coatings, with the aim of verifying whether the introduction of colloidal silver has introduced defects in the polyurethane matrix. Moreover, the optical stereomicroscope was used to assess the silver distribution into the polymeric matrix and to measure the thickness of the three series of coatings.

To evaluate the effect of silver on the durability of the coatings, considering their possible application in outdoor environments, the three series of samples were subjected to two accelerated degradation tests, simulating exposures in aggressive environments.

Cellulose fibers and lignin matrix represent the main components of wood: the hygroscopic groups of these materials make wood highly hydrophilic. Therefore, the presence of water or moist conditions can influence several mechanical feature of wood, as well as its dimensional stability [94, 95]. When exposed to water, the decay of wood is accelerated, as well as the growth of fungi and molds which are harmful to the durability of the wood itself [96]. One of the most used expedients to slow down the deterioration of wood is represented by coatings [97]. Thus, in this work the protective contribution of the polyurethane-based coating was analyzed, verifying the effect caused by the introduction of silver in the paint. The coated-wood plates were subjected to a climatic chamber exposure, undergoing continuous thermal changes. The test consisted of a succession of cycles of 6 hours at a temperature of +40 °C and relative humidity > 90%, followed by 6 hours at a temperature of -5 °C. The samples were monitored after 50, 100, 200, 300, 400 and 500 hours of exposure in the climatic chamber, through electronic microscope observation, to assess the possible influence of colloidal silver in reducing the durability of the composite organic coating. To limit the moisture absorption by the wood substrate, the edges of the samples were coated with a red spray acrylic paint, leaving uncovered a 4 x 4 cm^2 testing area of the samples. The performances of the three series of coatings were compared with the behavior of an uncoated wood sample, to study the effective insulating effect of the polyurethane-based paint. Furthermore, the effect of prolonged exposure to thermal changes on the adhesion of the coatings was assessed with the Cross Cut Test, following the ASTM D3359 standard [98], performed before and at the end of the test.

The ultraviolet radiation represents one of the most severe causes of degradation of organic coatings, capable of modifying their aesthetic features. Thus, the organic layers employed in outdoor applications are often characterized by means of accelerated degradation tests such as the UV-B exposure, to evaluate their durability. Polyurethane coatings were known for their poor resistance to solar radiation and especially to the UV component [99, 100]. However, several studies have been conducted to improve this aspect, through modifications of the formulations of the coatings [101] and introduction of particular additives [102, 103]. Similarly, silver particularly suffers exposure to ultraviolet radiation, undergoing degradation phenomena such as retention, dissolution, and oxidative aging [104, 105]. Furthermore, these reactions can be strongly influenced by temperature increases [106]. Thus, in order to study the behavior of the polyurethane-Ag coatings exposed to sunlight, the samples were tested in a UV-B chamber (313 nm) for 200 hours, employing an UV173 Box Co.Fo.Me.Gra (Co.Fo.Me.Gra, Milan, Italy), following the ASTM G154-16 standard [107]. The degradation of the coatings due to the UV-B exposure was monitored by FTIR infrared spectroscopy measurements and colorimetric analyses. The FTIR spectra were acquired with a Varian 4100 FTIR Excalibur spectrometer (Varian Inc., Santa Clara, CA, USA), to assess the chemical modifications of the polymeric matrix. The colorimetric analyses were carried out by means of a Konica Minolta CM-2600d spectrophotometer (Konica Minolta, Tokyo, Japan) with a D65/10° illuminant/observer configuration in SCI mode. Since the same wood tends to undergo severe degradation with solar

radiation [108, 109], the behavior of the three coatings was compared with the performance of a panel of poplar wood, to differentiate the possible causes of degradation observed in the different samples. Finally, to better analyse the behavior of the polyurethane-based paint, removing the influence of the wooden substrate, the three coatings were applied on a white substrate, immune to colour changes due to UV-B radiation. This white substrate was realized by spraying the Unimarc Smalto Seta white acrylic-based primer on a low-carbon steel panel, to get a layer of about 70 µm of thickness.

2.3.2 Evaluation of Antimicrobial Activity of Silver-Treated Wood Coatings

The experiments were conducted at the Laboratory of Hygiene, University of Cagliari, accredited UNI EN ISO /IEC 17025:2018 (General requirements for the competence of testing and calibration laboratories) according to ISO 22196: 2011 [93]. The tests involved the use of untreated samples made of wood with water-based paint (Ag0) and treated samples made of wood and water-based paints with 0.1% colloidal Ag (Ag01) as well as of wood with water-based varnish with 0.5% colloidal Ag (Ag05). All samples were disinfected by immersion in Chlorhexidine digluconate (0.02%) and Benzalkonium chloride (0.2%) for 10 minutes and subsequent ultraviolet (UV) radiation for 1 hour per side in a sterile tray inside a laminar flow hood [59, 110]. The antibacterial activity of these coatings was tested against Gram-positive *Staphylococcus aureus* strain ATCC 6538 and Gram-negative *Escherichia coli* ATCC 25922 (class II). The microbial suspensions were prepared from lyophilized pellets (according to EN1276) resuspended in Nutrient Broth medium. Concentration was determined by spectrophotometric reading (Agilent Technologies Cary 60). Bacteria were pre-cultured overnight at 35 ± 1 °C on NA plates and then inoculated in 10 ml of NB 1/500 until initial bacterial concentration of 1.5 10^8 cells/ml (McFarland standard 0.5). Then this suspension was diluted in sterile 1x PBS to obtain a suspension (inoculum) with an estimated bacterial concentration between 1.0 10^6 and 6.0 10^6 cells/ml, with a target concentration of 2.5 10^6 cells/ml. Colony forming units CFU/ml were determined by 10-fold dilution and plating on NA plates followed by overnight incubation at 35 ± 1 °C. The inoculum (100 µL) was applied to the three series of highly disinfected surfaces (25 mm 25 mm), and covered with polypropylene film (20 mm 20 mm). The three replicates of samples Ag0/T24, Ag01/ T24 and Ag05/T24 were incubated at 35 ± 1 °C for 24 h, at a relative humidity of 90%. The control sample Ag0/ T0, which represents the inoculation at T0, was processed immediately after direct contact with the bacteria. The recovery of bacterial cells from Ag0/T0 occurred by washing with 10 ml of sterile 1x PBS, vortexing for 1 min to detach them from the surface and after serial dilutions were included and incubated in PCA plate at 35 ± 1 °C for 24h for colony counting. After incubation for 24 h (T24), bacterial cells were recovered from the test samples (Ag01, Ag05) and from the untreated sample (Ag0) by adding 10 ml of sterile 1x PBS and vortexing for 1 min. After this step, 10-fold dilution were performed in 1x PBS and 1 ml of each sample was included in PCA plates and incubated at 35 °C for 24 and 48 h to enumerate viable bacteria. The bacterial colonies were counted according to the BS ISO 22196 protocol and expressed as:

$$N\ (cells/cm^2) = (100\ C\ D\ V)/A,$$

where N is the number of viable bacteria recovered for cm^2 for test sample, C number of colony forming units (CFU) determined by counting on agar plates for each group of samples, D is the dilution factor for the counted plates, V is the volume in mL of the bacteria recovery solution from the samples, A the surface of the cover film in cm^2.

The antibacterial activity of the treated surfaces was calculated by the following equation:

$$R = (Ut - U0) - (At - U0) = Ut - At,$$

where: U0 = $\log_{10}$ average of the number of viable bacteria recovered from the untreated surface immediately after inoculation; Ut = $\log_{10}$ mean of the number of viable bacteria recovered from the untreated surface after 24 hours of incubation; At = $\log_{10}$ mean of the number of viable bacteria recovered from the treated sample after 24 hours of incubation**.**

Finally, the LR microbial reduction index was calculated (ISO 20743: 2021 Textiles - Determination of antibacterial activity of textile products) as:

$$LR = P0 - PR \text{ where:}$$

P0 = $\log_{10}$ average of the number of viable bacteria inoculated at the start of the test; PR = $\log_{10}$ mean of the number of bacteria surviving at each time interval.

The % R reduction percentage is calculated as:

$$\%\ R = 100 \times (1 - 10^{-LR}).$$

Figure 1 exhibits the graphical abstract of the protocol ISO 22196:2011.

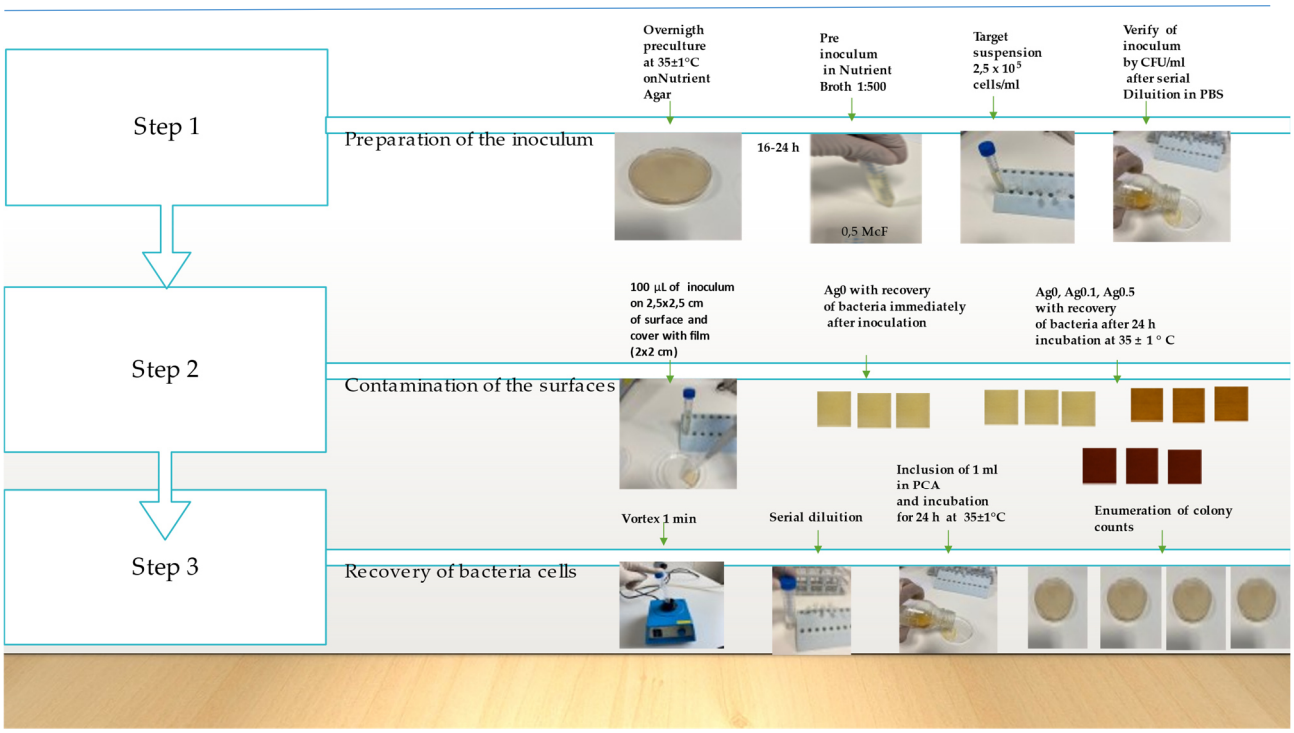

Figure 1: Graphical abstract of the protocol ISO 22196:2011. CFU, Colony-Forming Units; PBS, Phosphate-Buffered Saline; PCA, Plate Count Agar.

2.3.3 Evaluation of Fungicidal Activity of Silver-Treated Wood Coatings

Wood decay fungi are one of the main causes of wood degradation [82], even when the wood component is painted [83]. Among the various possible functional fillers for paints, silver has displayed good fungicidal activity, leading to an increase in the durability of paints and, consequently, of the wood itself [89, 90]. The evaluation of biological resistance of the coatings was evaluated with two fungal strains *C. puteana* Ebw 15 and *T. Versicolor* CTB 863, respectively a brown rot and a white rot that cause decay in service of wood products in all Europe. *C. Puteana* is the mandatory and representative fungus for natural and conferred resistance by a treatment for European standards belongs to CEN TC 38 Durability of wood and derivate. *T. versicolor* is a fungus for particular risks and is recommended for outdoor applications. The method was in accordance with ENV 12038 [111] with some modifications due to the duration of trial, only 13 weeks instead of 16, and only two fungi instead of three.

The method was carried out placing the three series of samples (completely coated by dipping process) in contact with a pure mycelium of above described fungi. The panels, introduced in container with a completely developed fungus, respectively brown or white rot, were maintained in a conditioned room (22 ± 2 °C - 75 ± 5% relative humidity) for 13 weeks. Then, the panels were carefully cleaned from mycelium and weighted after 24 h at 103 °C in oven. The determination of biological resistance was expressed in terms of mass loss percentage. The standard ENV 12038 considers a treatment as resistance if the samples exhibit no more of 3% of mass loss. Untreated wood panels were used as 'control' samples, to validate the test. In fact, the experiment is considered as robust if the untreated samples exhibit a minimum of 20% of mass loss.

3. Results and discussion

3.1 Colloidal silver and coatings morphology

The second paint deposition of sample Ag01 and sample Ag05 took place by introducing colloidal silver into the polyurethane matrix. The commercial colloidal silver product appears in the form of gray granules, ranging in size from a few μm up to over 200 μm. **Figure 2** shows the morphology of the Ag powders, acquired by SEM observations. A recent work [112] has demonstrated the high solubility of this product in water and consequently its reliability to be used as an additive in water-based paints. The colloidal silver granules shown in **Figure 2**, once introduced in water, tend to partially dissolve, to become substances smaller than μm, forming a homogeneous suspension.

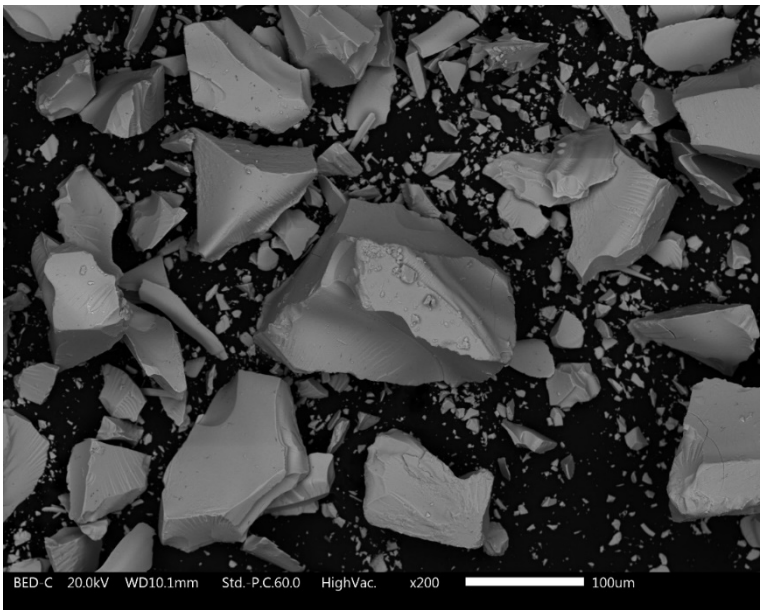

Figure 2: colloidal silver acquired by SEM.

Once the colloidal silver granules are introduced in water, they produce an orange colour suspension, the hue of which varies according to the concentration of dispersed powder [112]. Consequently, once the transparent polyurethane-based paint is diluted with the Ag-aqueous suspension, its appearance also changes radically. From the starting clear colour, the paint turns orange and red, adding 0.1 wt.% and 0.5 wt.% of colloidal silver, respectively. Thus, the appearance of the three series of coatings is very different, as can be appreciated in **Figure 3**, acquired with the optical stereomicroscope.

Figure 3 shows both the cross sections (a, c, e) and the top-view (b, d, f) of the surfaces of the three series of coatings. The cross sections of sample Ag01 and sample Ag05, exhibited in **Figure 3c** and **Figure 3e**, respectively, highlight the two layers that make up the protective systems. The coloured paint used in the second deposition differs visibly from the first transparent layer. The first deposition produced a layer with a thickness of about 50 μm. Otherwise, as the paint used in the second deposition was diluted with the Ag-aqueous suspension, the thickness of the second layer is slightly lower, equal to about 40 μm. Ultimately, the thicknesses of the three coatings vary between 100 μm for sample Ag0, to approximately 85-95 μm of sample Ag01 and sample Ag05.

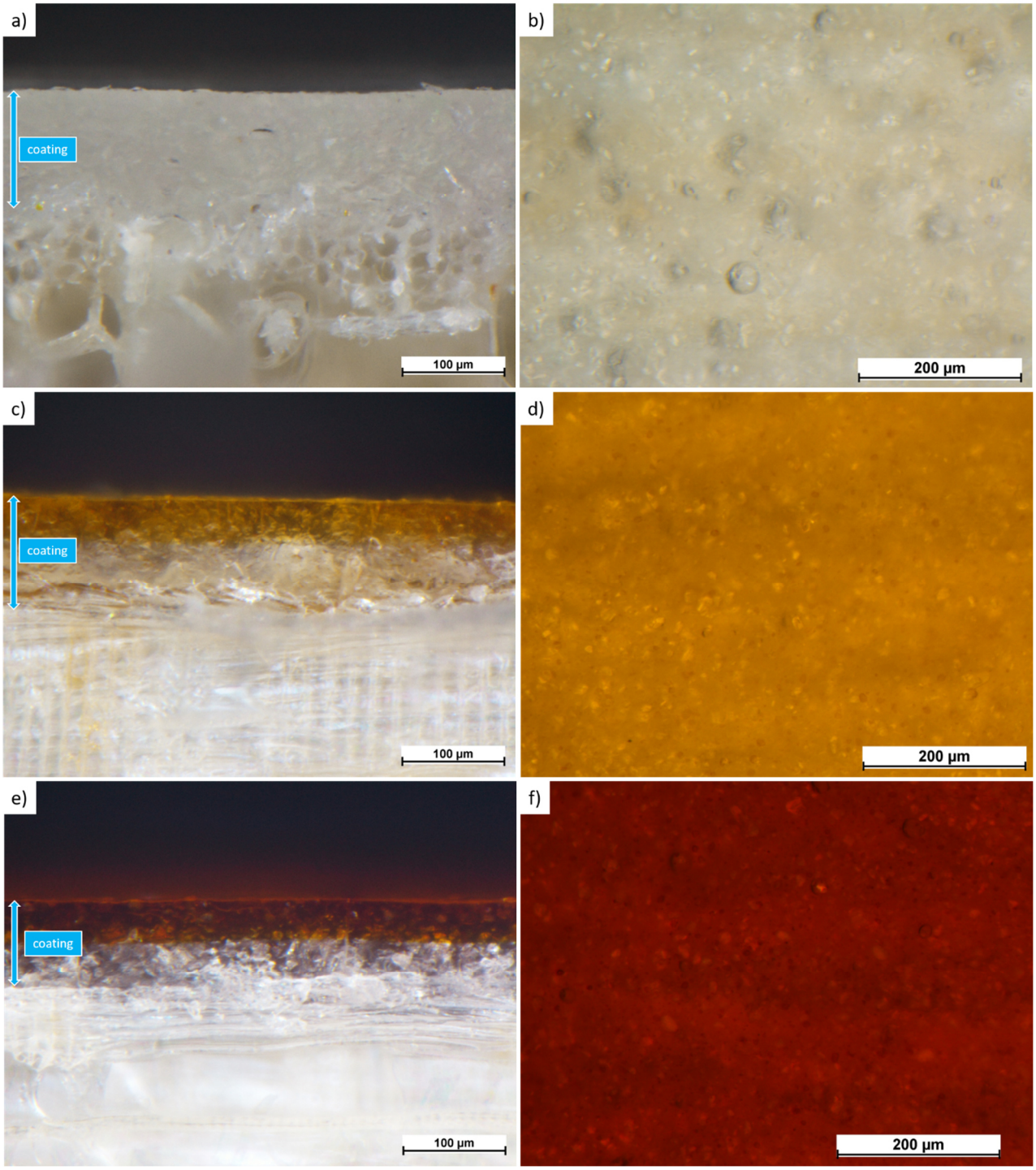

Figure 3: optical microscope micrographs of sample Ag0 a) cross section and b) top-view, sample Ag01 c) cross section and d) top-view and sample Ag05 e) cross section and f) top-view.

Apart from the decrease in thickness, the addition of colloidal silver in the polyurethane paint does not produce defects in the composite layer. The surfaces of sample Ag01 and sample Ag05 (**Figure 3d** and **Figure 3f**, respectively) appear compact, free of bubbles or other macroscopic defects. The colour is homogeneous over the entire surface, demonstrating the excellent dispersion of Ag granules in the aqueous suspension used to dilute the polyurethane paint. Although wood is appreciated for its specific aspect, often the market requires wood paints that possess peculiar aesthetic features and eye-catching colours, able to provide the wooden product with innovative

appearances [31]. Thus, colloidal silver could be used as an alternative pigment, whose low concentrations are capable of producing intense orange-red colouring in transparent paints.

3.2 Sample exposure to different aggressive environments

The high colouring efficiency and good solubility in aqueous suspension make colloidal silver an ideal candidate as a multifunctional pigment for water-based paints. However, it is necessary to verify the impact of this type of filler on the protective performance of the paint. Therefore, the samples were subjected to accelerated degradation tests, undergoing continuous thermal changes and exposure to UV-B radiation.

3.2.1 Climatic chamber exposure

To avoid dimensional instability phenomena due to the penetration of moisture from the sides of the samples, the edges were coated with a red spray acrylic paint, as can be seen in **Figure 4**, which shows the evolution over time of the appearance of the samples. The aspect of the surfaces does not change during the exposure in the climatic chamber. The three series of samples reveal a constant color over time, as well as the absence of macroscopic defects. Therefore, the paint seems to have adequately protected the substrate, providing good durability. At the same time, silver does not undergo particular degradation, offering good resistance to thermal changes. From a macroscopic point of view, even the pure wood sample does not exhibit physical decay following the test, thanks to its good compactness.

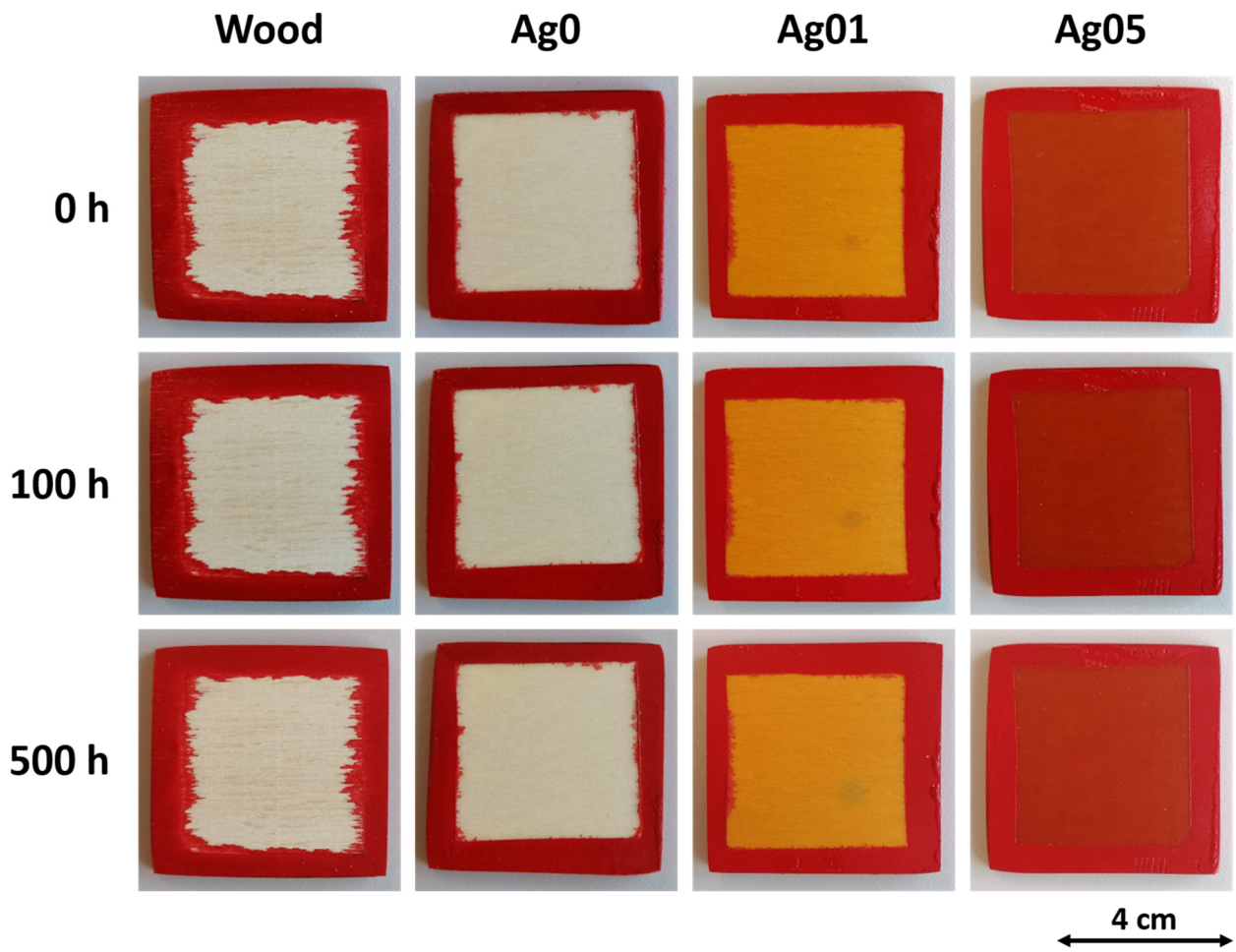

Figure 4: evolution of the appearance of the samples during the exposure to climate chamber.

Differently, the exposure in the climatic chamber had consequences on the geometric stability of the four sample series at a microscopic level, as can be appreciated from the images in **Figure 5**, acquired by SEM. **Figure 5a** and **Figure 5b** highlight a crack developed in the coating of sample Ag01, as a consequence of exposure in the climatic chamber. The surface around the defect does not exhibit a critical point, which may have acted as a crack initiation. However, this crack represents a highly dangerous element for the integrity of the coating itself, but also for the durability of the wooden product. Considering the dimension and depth of the crack, which extend over 1000 µm and over 20 µm, respectively, it is probable that the defects is so severe as to reach the wood substrate. **Figure 5c** shows an important phenomenon observed in the uncoated wood sample. While the visual inspection did not reveal any particular morphological changes in the wood, the SEM observations showed the consequences of the absorption of moisture by the sample. The high levels of humidity and the continuous thermal changes put at risk the structural integrity and dimensional stability of the poplar wood, with consequent detachment and raising of the fibers. Although organic coatings act as insulating and protective layers, their polymeric matrix possesses intrinsic porosity. Therefore, the moisture is able to leach through the coating over time, until it reaches the wooden substrate. The crack shown in **Figure 5a** and **Figure 5b** is the consequence of the swelling of the wooden substrate, which occurred due to the inevitable absorption of moisture.

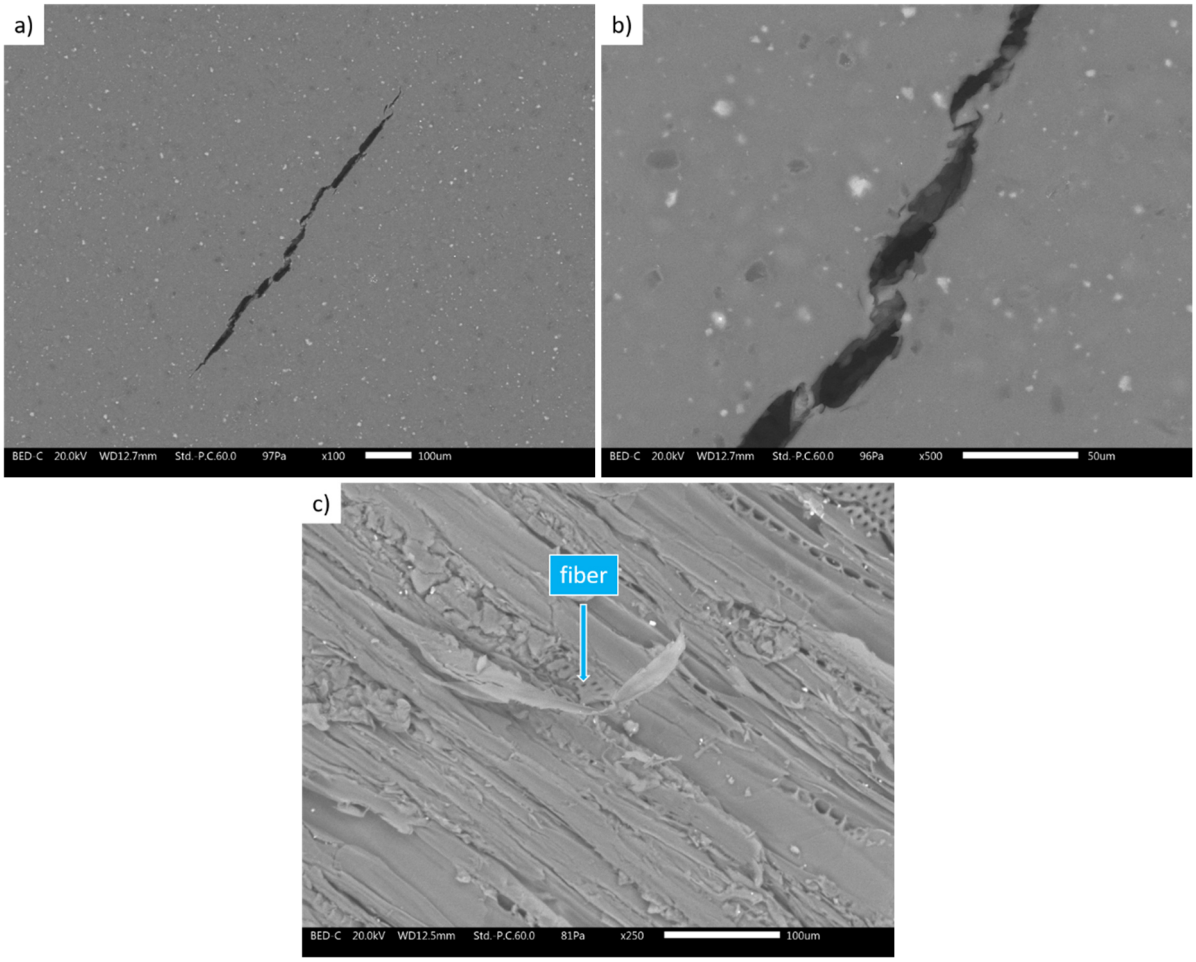

Figure 5: a) SEM micrograph of a crack observed in coating Ag01 after the climatic chamber test. b) magnification with detail of the fracture surface. c) detachment of the fiber in the wood sample due to swelling owing to the humidity of the climatic chamber test.

Although these cracks represent a dangerous phenomenon, only a few similar defects have been analysed in the three coating series, highlighting a good protection offered by the polyurethane-based layers. At the same time, it was not possible to differentiate the behavior of the three coatings, suggesting that silver does not affect the protective performance of the paint.

Conversely, colloidal silver appears to have influenced the adhesion levels of the paint to the wood, as highlighted in **Figure 6**, which shows the Cross Cut Test results on the surface of three series of coatings before and after exposure in climatic chamber. Before the accelerated degradation test, all the three coatings possess good adhesion, equal to value 4B considering the standard rating [98]. The classification 4B represents a percentage of less than 5% of the coating surface removed following the test. On the other hand, following the 500 h of exposure in the climatic chamber, the three coatings revealed different adhesion performances. The visual results reflect grade 3B, 2B and 0B for sample Ag0, sample Ag01 and sample Ag05, respectively. Obviously, the addition of silver affects the degradation processes in the climatic chamber. A greater penetration of moisture in the Ag-polyurethane coatings could be correlated to a lower thickness of the layer of the second deposition. However, sample Ag01 and sample Ag05 possess comparable thickness, but different levels of adhesion. The results suggest a greater percolation of water as a function of the increase

in silver amount. Indeed, it has already been demonstrated how the addition of colloidal silver in paints can represent a cause of discontinuity in the polymeric matrix, decreasing the barrier effect and the protective performance of the composite layer [112].

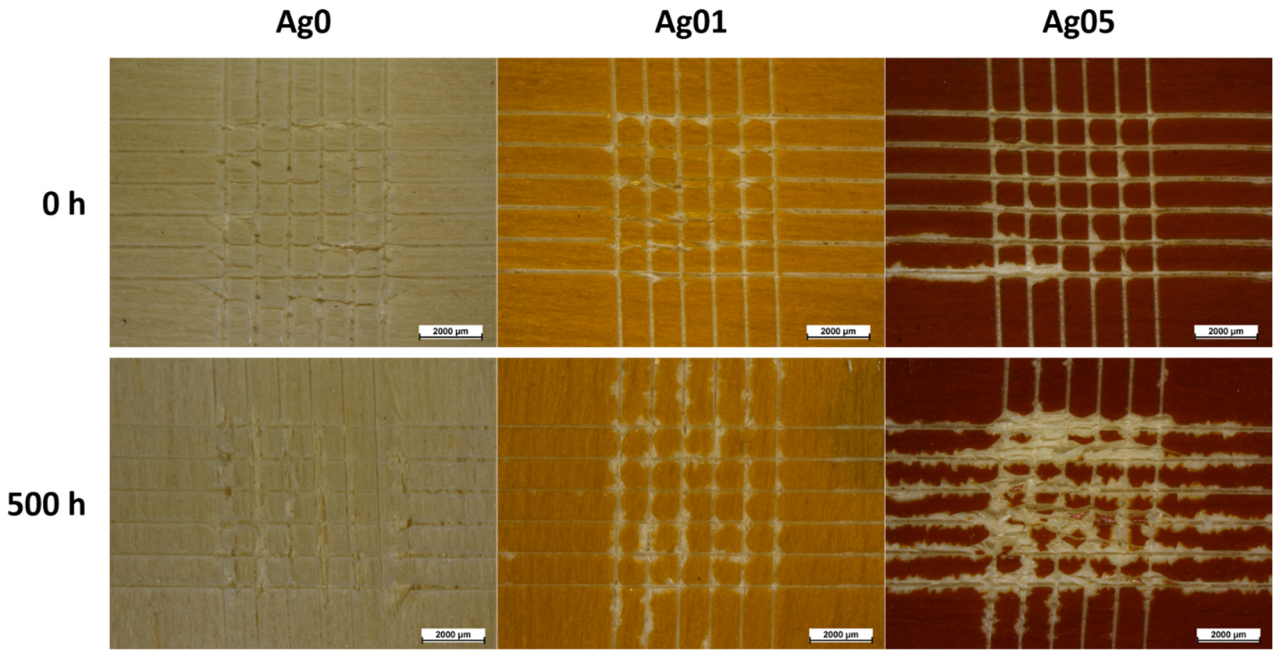

Figure 6: Cross Cut Test results before and after exposure in climatic chamber, observed with stereomicroscope.

Figure 7 shows some details of the test output for the three series of samples. In some cases, the peeling takes place at the interface between the two layers. However, it is more common to observe the complete peeling of the coating, which reveals the wooden substrate.

The negative effect of silver was not appreciated by the simple observation of the defectiveness of the coating, but it was revealed by monitoring the levels of adhesion following thermal changes with high concentrations of humidity. This study demonstrates how visual and microscopic observations do not always highlight the real effect introduced by the fillers in modifying some properties of the coating. The absence of defects in the layer matrix does not necessarily reflect the integrity of the coating itself. In this case, the colloidal silver introduced in the second deposition negatively affects the barrier performance of the top-layer. The first layer, made with pure polyurethane-based paint, is capable of limiting the phenomena of dimensional instability of the wooden substrate, but it is not sufficient to maintain high adhesion values after exposure to high humidity environments. Consequently, the addition of colloidal silver is not recommended for paints employed in outdoor applications, subject to possible variations in temperature and humidity. However, to confirm this hypothesis, the samples were characterized by exposure to UV-B radiation.

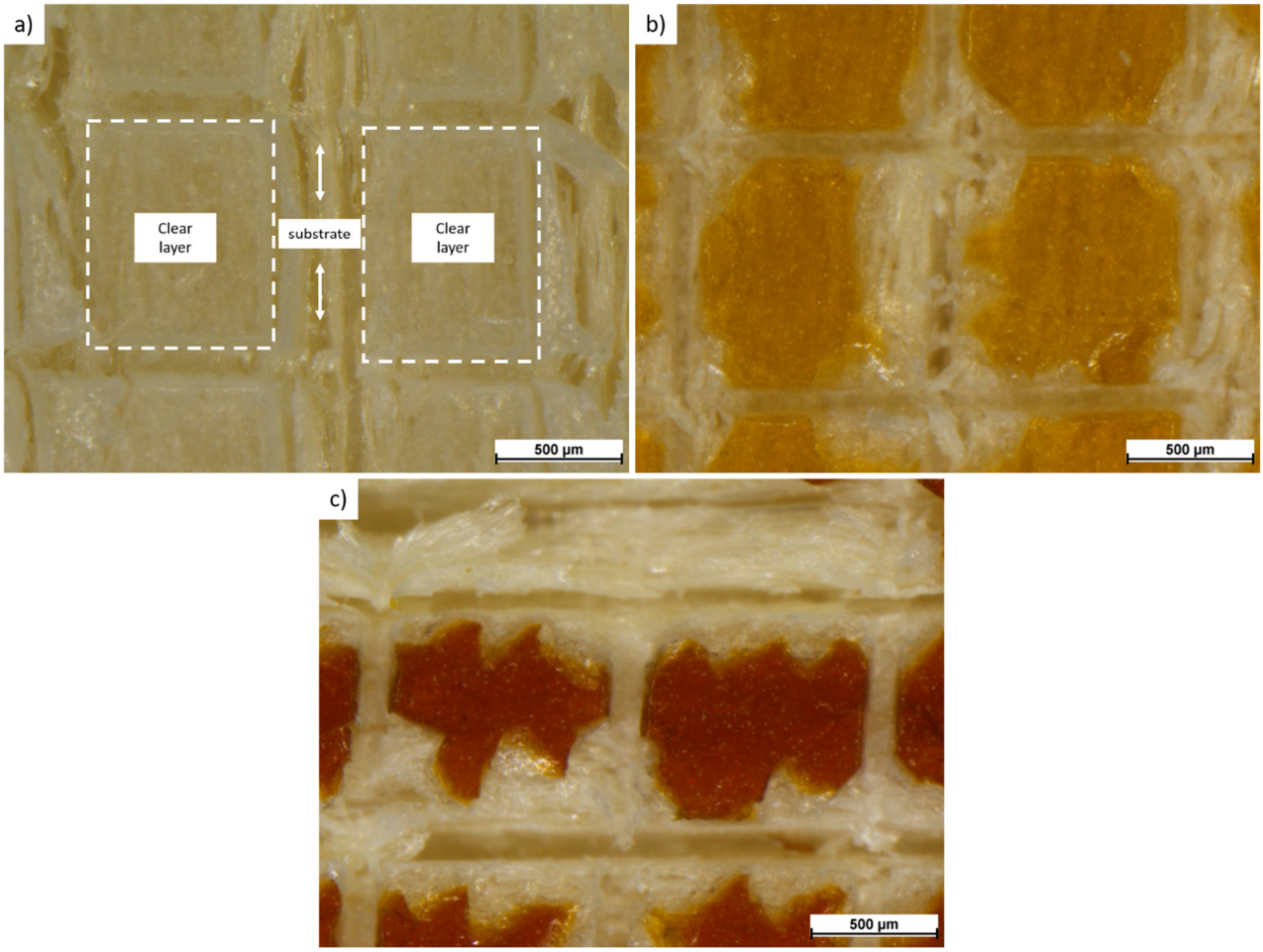

Figure 7: optical microscope micrographs of details of the Cross Cut Test results after exposure in climatic chamber of a) sample Ag0, b) sample Ag01 and c) sample Ag05.

3.2.2 UV-B exposure

Figure 8 shows the evolution of the FTIR spectra of the four samples (coated and uncoated wood) during the exposure to UV-B radiations. **Figure 8a** reveals the spectra of the poplar wood panel, in which it is possible to appreciate the absorption band between 3300 and 3400 cm^{-1} of the stretching vibration of the -OH group [113] and the stretching region between 2800 to 3000 cm^{-1} associated with the -CH group of cellulose, hemicellulose, and lignin [114]. The intense peak at 1029 cm^{-1} is associated to the typical C-O-C stretching vibrations of cellulose [115], the peak at 1233 cm^{-1} is representative of C-O stretching, while the band at 1460 cm^{-1}, 1502 cm^{-1} and 1592 cm^{-1} are attributed to C-H deformation vibration, aromatic skeletal vibration and C=C benzene ring vibration of lignin, respectively [116, 117]. Finally, the band at 1737 cm^{-1} is assigned to the stretching vibrations of the unconjugated C=O group and specific moieties of the polymeric chains present in the wood, such as esters [118]. The evolution of the spectra highlights an increase in the signal from the peak at 1737 cm^{-1} at the expense of a reduction in the signal at 1233 cm^{-1}. The analyses show an actual deterioration of the wood sample, whose cellulose has undergone an alteration of its chemical structure.

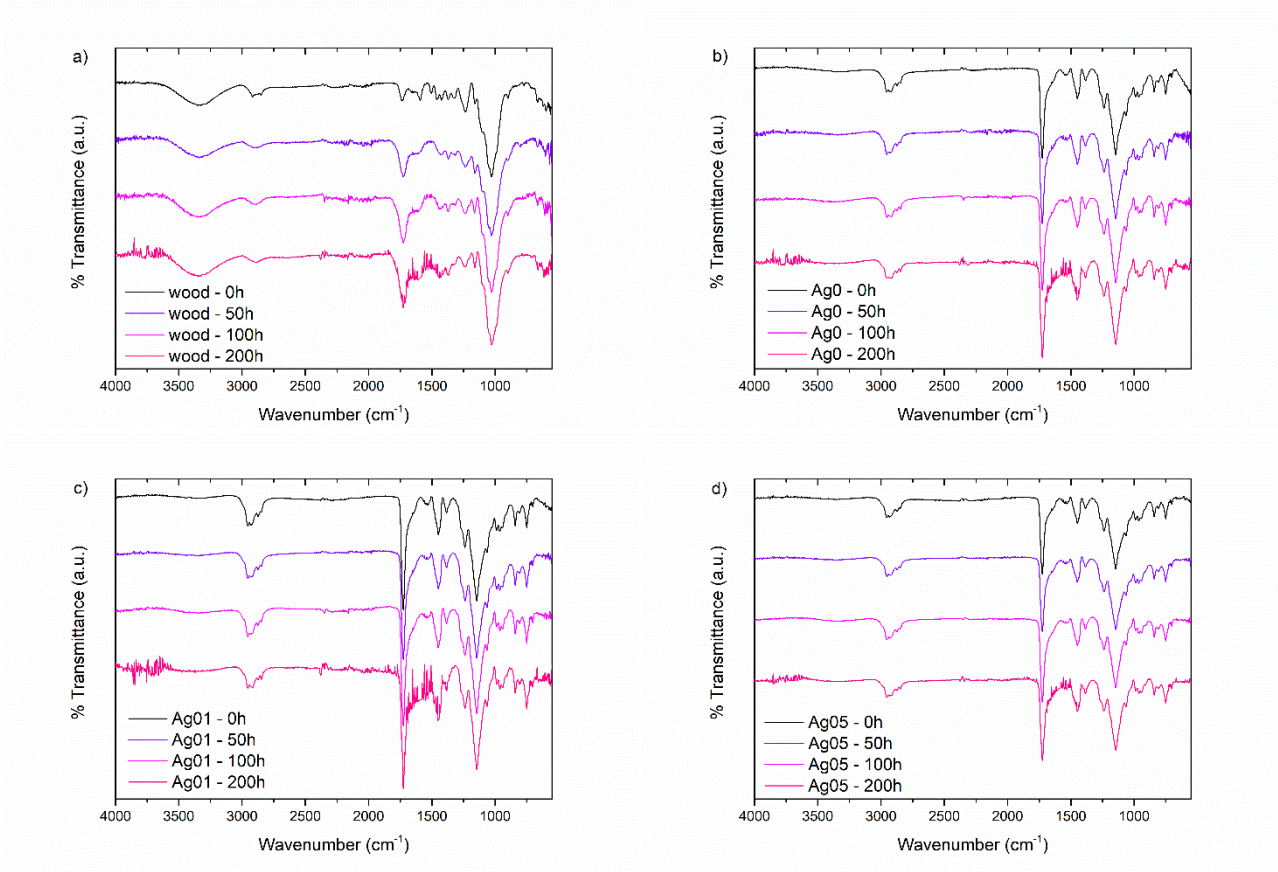

Figure 8: evolution of the FTIR spectra of a) the wood sample, b) coating Ag0, c) sample Ag01 and d) sample Ag05, during the exposure to UV-B radiation.

In contrast, the three coated samples exhibit very similar FTIR spectra (**Figure 8b, 8c, 8d**), which do not vary during exposure to UV-B radiation. The signal of the wood substrate disappears, due to the covering effect of the paint, while the typical peaks of polyurethane-based paints emerge. The slight absorbance at 3349 cm^{-1} is associated to the stretching of the NH bond, as characteristic of urethane and urea groups. The band at 2930 cm^{-1} is representative of the alkane -CH stretching vibration, while the intense peak at 1725 cm^{-1} represents the typical carbonyl absorption band, with a shoulder at 1658 cm^{-1} attributed to the urethane and urea carbonyl groups. The peaks at 1448 cm^{-1} and 1238 cm^{-1} represents the C-N stretching and N-H bending. The signal at 1145 cm^{-1} refers to the coupled C-N and C-O stretching vibrations, and the 963 cm^{-1} is correlated to the ester C-O-C symmetric stretching vibration [119]. The spectra of the three series of coatings are not affected by the presence of colloidal silver.

Ultimately, FTIR analyses suggest a good durability of the three polyurethane-based coatings, whose chemical structure is not modified following UV-B radiation. However, the appearance of the samples varies significantly during the test, as evidenced by the micrographs in **Figure 9**.

Figure 9: evolution of the appearance of the samples during the exposure to UV-B radiation.

The degradation of the chemical structure of the cellulose and lignin constituting the poplar wood results in a clear darkening of the surface of the poplar panel. Sample Ag0 shows a very similar behavior: since the paint is transparent, the appearance of the sample is strongly influenced by the aspect of the wood substrate. The two Ag-containing coatings also undergo a darkening phenomenon: this effect is more evident in sample Ag01, whose starting color is lighter, while it is less emphasized in the top-layer of sample Ag05, whose initial color is already quite dark.

To better highlight this behavior, **Figure 10** shows the total colour variation of the samples, ΔE, monitored during exposure to UV-B radiation. According to the ASTM E308-18 standard [120], ΔE is calculated as follows:

$$\Delta E = [(\Delta L^*)^2 + (\Delta a^*)^2 + (\Delta b^*)^2]^{1/2}$$

where the colorimetric coordinates L*, a* and b* represents the lightness (0 for black and 100 for white objects), the red-green coordinate (positive values are red, negative values are green), and the yellow-blue coordinate (yellow for positive values, blue for negative values and 0 as neutral parameter), respectively.

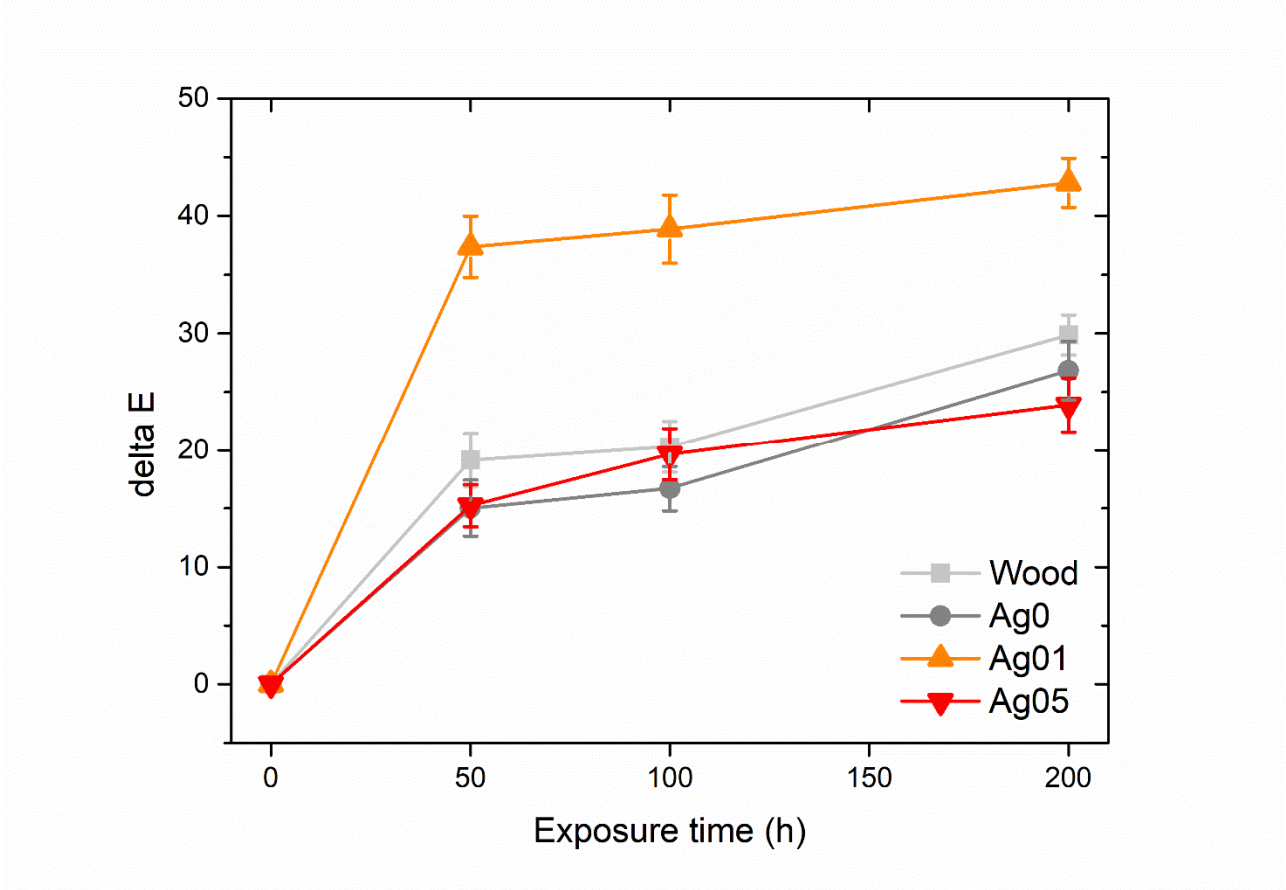

Figure 10: total color variation during UV-B exposure.

The poplar panel exhibit a fast and sensible colour change during the first 50 h of exposure. Subsequently, the ΔE value continues to grow almost linearly until the end of the test, reaching values of about 30. This colour variation was easily noticed by the visual inspection exhibited in **Figure 9**, as the human eye is capable to appreciate a colour variation ΔE ≥ 1 [121]. Sample Ag0 shows an almost identical trend, simply shifted to about 5 lower ΔE values. Indeed, the appearance of the sample coated with the transparent paint is affected by the decay of the wooden substrate, but this degradation is limited by the presence of the protective polyurethane layer. As previously described, the colour change is more evident in sample Ag01, whose final ΔE almost reaches a value of 45. Evidently, silver also contributes to the colour change of the composite coating, due to its poor resistance to ultraviolet light [104, 106]. This phenomenon is actually less marked in sample Ag05, despite the fact that the coating possesses a higher amount of silver. However, the starting hue is already so dark that it is difficult to appreciate a further colour change due to the darkening of the sample.

However, to better analyse the behavior of the polyurethane-based paint, removing the influence of the wooden substrate, the three coatings were sprayed on the Unimarc Smalto Seta white acrylic-based primer, immune to colour changes due to UV-B radiation, deposited on the carbon steel panel. The white substrate and the three polyurethane coated samples were subjected to UV-B exposure, monitoring the variation of the colour coordinates.

Figure 11 exhibits the evolution of the colour coordinates during the test. The colour coordinates a*, b* and L* of the white primer do not undergo any variations, confirming the non-susceptibility of the acrylic substrate to UV-B radiation. The employ of the white primer made it possible to remove the influence of the wood substrate, which was highly sensitive to ultraviolet radiation. Sample Ag0 shows a slight decrease in a*, correlated with an increase in b*. This almost negligible variation demonstrates that the colour change ΔE of sample Ag0 observed previously was mainly due to the severe decay of the wooden substrate. Therefore, the polyurethane paint expresses high durability and low sensitivity to UV-B radiation. The darkening highlighted by the two coatings containing Ag is due, rather than to a decrease in the L* parameter, representative of the brightness of the layer, to a significant decrease in both the a* and b* parameters. The real difference between sample Ag01 and sample Ag05 lies in the high starting value of the coordinate b*, tending to yellow, of the former: the degradation of silver leads to such a severe decrease in the value of b* that it affects the entire ΔE of sample Ag01. Otherwise, the final b* value of sample Ag05 is even lower, but the total variation is about 15 points, against almost 30 for sample Ag01. As a matter of fact, the values of b* of sample Ag05 are very low from the beginning, and almost reach 0 at the end of the test. Consequently, the colour change ΔE of the coating containing 0.5 wt.% of colloidal silver, although it is evident, is less pronounced than for sample Ag01.

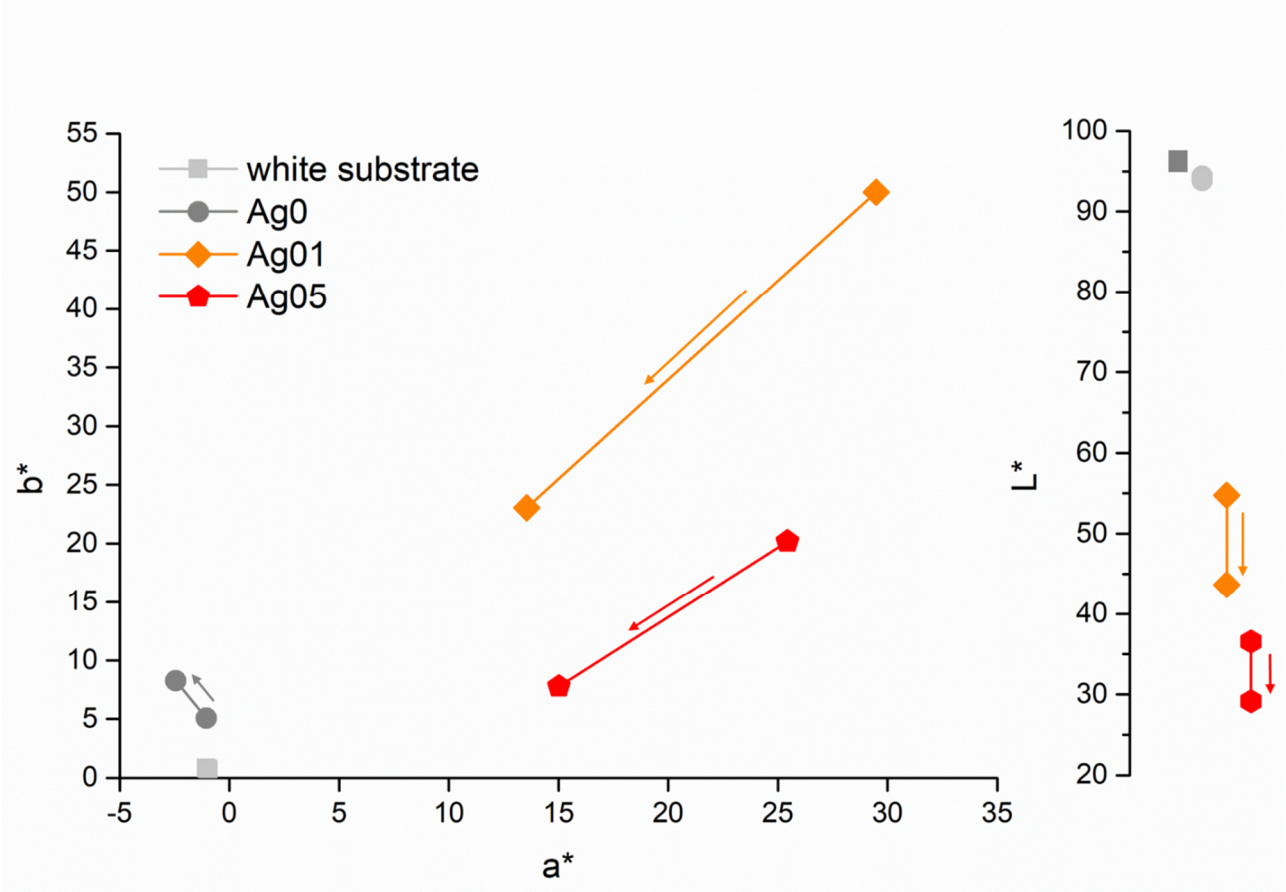

Figure 11: variation of the parameters a, b* and L* during the first 50 h of exposure to UV-B radiation.*

Ultimately, the four series of samples exhibited a noticeable change in appearance due to exposure to UV-B radiation. The poplar panel undergoes a natural degradation of lignin and cellulose, while the polyurethane-based paint is not influenced by UV-B light: thus, the colour change of the Ag0 sample is mainly due to the decay phenomena of the wooden substrate. On the contrary, sample Ag01 and sample Ag05 reveal a strong colour change which is largely due to the chemical-physical degradation of the colloidal silver.

Therefore, despite possessing good resistance to ultraviolet radiation, the polyurethane-based paint is not recommended for outdoor applications, as it is transparent. At the same time, the application of colloidal silver further enhances the colour change of the component, due to the oxidation phenomena of Ag. The exposure to UV-B radiations represents a particularly aggressive test, which is not fully representative of the natural exposure to sunlight, in terms of frequency and intensity of the radiation. However, the severe degradation of silver inevitably directs this type of composite coatings to application on wooden products designed for interior design.

3.3 Antibacterial Activity of Silver-Treated Coatings

The presence of materials with biocidal activity is essential to prevent bacterial biofilms that could inhibit these properties. Especially when used in healthcare-related environments, biocidal surfaces represent an ambitious goal. Organizational problems associated with constant sanitization

protocols, careless behavior by the staff in charge of sanitization and phenomena of development of bacterial resistance [122] could be significantly contained. This can be done by using the characteristics of broad-spectrum antibacterial activity of silver [79, 82, 83] and introducing colloidal silver into the polyurethane matrix into wooden surfaces. In fact, their ability to inhibit any contamination was evaluated using the BS ISO 22196 protocol [93] with two target microorganisms *E. coli* and *S. aureus*. The conditions required for the validity of the test were always satisfactory (**Table 2**). Tests conducted in triplicate on two samples at different concentrations of silver (Ag01 and Ag05) showed comparable results. The growth of the target microorganisms on the treated surfaces compared to the untreated ones was completely inhibited at 24h, confirming the antibacterial activity of the Ag also on this type of surface, as reported in previous works for different types of layers containing silver [74]. The average value of the antibacterial activity R of the surfaces was found to be equal to 3.98 in the case of *E. coli* and 3.78 in the case of *S. aureus*, which correspond to a percentage of reduction in the number of viable bacteria compared to the initial inoculation ones equal to 98.99% and 99.98%, respectively**.**

	E.coli			***S.aureus***		
	r1	**r2**	**r3**	**r1**	**r2**	**r3**
Inoculum (CFU/ml)[a]	$5,6x10^6$	$5,6x10^6$	$5,6x10^6$	$3,8x10^6$	$3,8x10^6$	$3,8x10^6$
Recovery counts untreated Ag0/T0	$1,4X10^4$	$1,2X10^4$	$1,6X10^4$	$1,1X10^4$	$1,0X10^4$	$1,0X10^4$
Validity recovery counts Ag0/T0[b]	0,03	0,03	0,03	0,01	0,01	0,01
Recovery counts untreated Ag0/T24[c]	$1,2X10^4$	$8,8X10^3$	$1,0X10^4$	$1,2X10^4$	$1,2X10^4$	$1,2X10^4$
Recovery counts treated Ag01/T24	<1	<1	<1	<1	<1	<1
Recovery counts treated Ag05/T24	<1	<1	<1	<1	<1	<1
Antibacterial activity (R)	4,01	3,94	4	3,73	3,73	3,88

Table 2: Antibacterial activity of Ag01 and Ag05 treated against E.coli and S.aureus.

a= range $1,0x10^6$ CFU/ml - $6,0x10^6$ CFU/ml; Conditions for a valid test**: b**=(Lmax-Lmin)/Lmean≤0,2; **c**>$6,2x10^1$ cells/cm^2

3.4 Fungicidal Activity of Silver-Treated Coatings

Figure 12 exhibits the outcome of the exposure test. The results of the three painted samples are compared with the loss of mass expressed by the ‘control’ panel, consisting of an unpainted wood sample. The ‘control’ panel confirmed the validity of the test, as it revealed a mass loss greater than

the minimum required by the standard (20%) for both tested fungi. The three series of painted samples showed a significantly lower loss of mass compared to the wooden panel, highlighting a functional barrier effect against the attack of the two types of fungi.

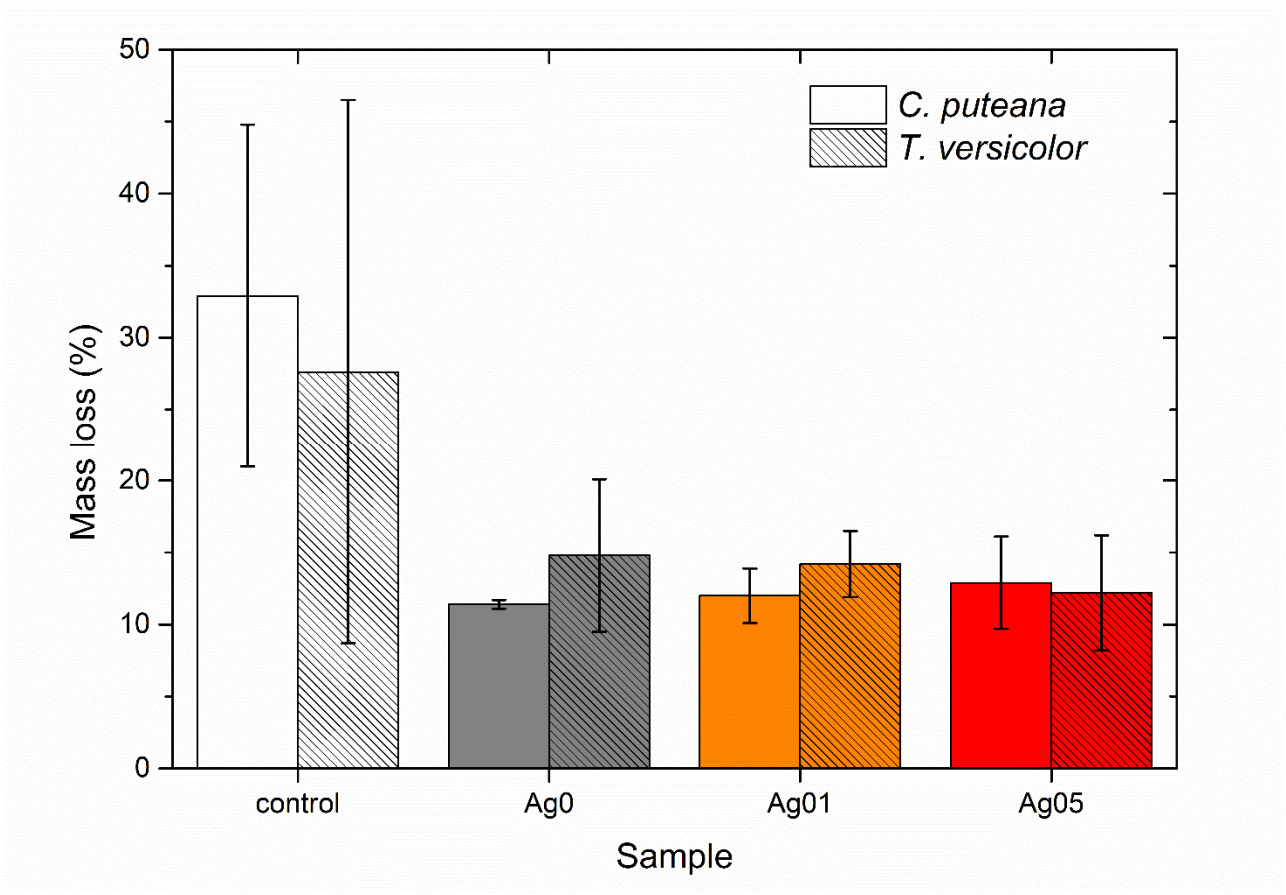

Figure 12: mass loss of the samples after 13 weeks of contact with C. puteana and T. versicolor fungi.

However, the behavior of the three series of painted samples is comparable to each other. This outcome demonstrates that the presence of colloidal silver was not sufficient to significantly improve the fungal resistance of the water-borne paint. This phenomenon is closely related to the low amount of silver added to the polyurethane-based coating. The surfaces of sample Ag01 and Ag05 were analysed with SEM-EDXS observations, which show a silver element concentration ranging from 0.23 to 1.22 wt.%, respectively (the EDXS spectra are presented in the Supplementary material). The works present in the literature show an effective fungicidal activity of silver nanoparticles when the Ag amount added to the organic coating is higher than 5.00 wt.% [89, 90]. Thus, the quantity of colloidal silver used in this study is probably not sufficient to reduce the attack of fungi, while the fungicidal activity is mainly exerted by the water-borne paint.

Nevertheless, the presence of colloidal silver did not cause an increase in mass loss. Although silver represents a discontinuity in the polyurethane matrix, it does not seem to facilitate the penetration of the fungi inside the paint, compromising the coating barrier functions.

Ultimately, colloidal silver did not show evident fungicidal activity, due to low Ag quantities, but at the same time it did not prejudice the protective properties of the polyurethane paint against these eukaryotic organisms.

4. Conclusions

This work shows the effects introduced by silver-based fillers in a water-based wood paint. Colloidal silver is suitable for use as a multifunctional pigment, as the appearance of the paint varies considerably according to the quantity of silver-based filler introduced into the polyurethane matrix.
The behavior of the paint in the climatic chamber is not affected by the presence of silver, which does not suffer from exposure to particular temperature changes. However, silver-based fillers exhibited significant oxidation phenomena when exposed to UV-B radiation, changing the appearance of the wood paint. The paint does not undergo chemical degradation, and ensures good protective performance, but the aesthetic decay is evident and irreversible.
In order to confirm the multifunctional contribution of the silver-based filler, the antibacterial activity of the samples was evaluated in accordance with ISO 22196: 2011 These studies highlight a remarkable antibacterial effect as evidenced by a medium high R against infectious agents. This occurs after 24 hours from the experimental contamination with these surfaces, thus showing a reduction of about 99.99% of viable bacteria. The results were the same for the two bacterial strains used, that is, *S. aureus* and *E. coli,* and for the two concentrations of silver in the two types of surfaces. Further future studies on their "shelf life" could better outline the extent of their protection, hence highlighting the "Expiry date" as it happens for other products.
Finally, the presence of colloidal silver did not improve the fungicidal activity of the polyurethane-based paint, as the samples Ag01 and Ag05, in contact with the fungi *Coniophora puteana* and *Trametes versicolor,* did not show a significant decrease in mass loss. This behavior is mainly due to the low concentration of silver introduced into the paint, which is not sufficient to introduce an internal biocide effect: protection from fungi is therefore only provided by the physical barrier effect of the paint. However, the silver did not compromise the protective performance of the paint, as it did not facilitate the penetration of fungi into the polymer matrix.
Ultimately, this work demonstrates how colloidal silver can be used as a functional pigment in wood paint, capable of modifying the appearance of the coating, improving its antibacterial performance, without negatively affecting its protective performance. However, these multifunctional paints are not suitable for outdoor applications, due to the high tendency of silver to oxidize when exposed to UV-B radiation, while the colloidal filler is not sufficient, in limited concentrations, to improve the fungicidal activity of the polyurethane coating.

CRediT author statement

Massimo Calovi: Conceptualization, Methodology, Validation, Investigation, Data Curation, Writing - Original Draft. **Valentina Coroneo:** Methodology, Investigation, Data Curation, Writing - Original

Draft. **Sabrina Palanti:** Methodology, Investigation, Data Curation, Writing - Original Draft. **Stefano Rossi:** Resources, Writing - Review & Editing, Supervision, Project administration.

Acknowledgments

The authors greatly acknowledge the contributions of Massimo Nava (ICRO Coatings S.p.A., Bergamo, Italy) and Umberto Dainese (San Marco Group, Venice, Italy) regarding the paints supply. The publication was created with the co-financing of the European Union – FSE-REACT-EU, PON Research and Innovation 2014-2020 DM1062/2021.

References

[1] T. Pakarinen, Success Factors of Wood as a Furniture Material, Forest Products Journal, 49 (1999).
[2] G.C. Foliente, R.H. Leicester, C.-h. Wang, C. Mackenzie, I. Cole, Durability design for wood construction, Forest products journal, 52 (2002) 10-19.
[3] G. Wimmers, Wood: a construction material for tall buildings, Nature Reviews Materials, 2 (2017) 1-2.
[4] C. Jia, C. Chen, R. Mi, T. Li, J. Dai, Z. Yang, Y. Pei, S. He, H. Bian, S.-H. Jang, J.Y. Zhu, B. Yang, L. Hu, Clear Wood toward High-Performance Building Materials, ACS Nano, 13 (2019) 9993-10001.
[5] J. Ratnasingam, F. Ioras, The sustainability of the Asian wooden furniture industry, Holz als Roh-und Werkstoff, 61 (2003) 233-237.
[6] H. Bo, G. Hongwu, L. Guan, L. Yi, The application of technical wood in modern interior decoration, Furniture & Interior Design, 4 (2012) 14-15.
[7] J. Hao, X. Wu, G. Oporto, W. Liu, J. Wang, Structural analysis and strength-to-weight optimization of wood-based sandwich composite with honeycomb core under three-point flexural test, European Journal of Wood and Wood Products, 78 (2020) 1195-1207.
[8] J.K. Kim, K. Pal, Recent advances in the processing of wood-plastic composites, (2010).
[9] J. Salazar, J. Meil, Prospects for carbon-neutral housing: the influence of greater wood use on the carbon footprint of a single-family residence, Journal of Cleaner Production, 17 (2009) 1563-1571.
[10] L.A. Lowden, T.R. Hull, Flammability behaviour of wood and a review of the methods for its reduction, Fire science reviews, 2 (2013) 1-19.
[11] A.J. Stamm, Thermal degradation of wood and cellulose, Industrial & Engineering Chemistry, 48 (1956) 413-417.
[12] M. Borrega, P.P. Kärenlampi, Effect of relative humidity on thermal degradation of Norway spruce (Picea abies) wood, Journal of Wood Science, 54 (2008) 323-328.
[13] L. Tolvaj, C.-M. Popescu, Z. Molnar, E. Preklet, Effects of air relative humidity and temperature on photodegradation processes in beech and spruce wood, BioResources, 11 (2016) 296-305.
[14] D.N.S. Hon, S.T. Chang, Surface degradation of wood by ultraviolet light, Journal of Polymer Science: Polymer Chemistry Edition, 22 (1984) 2227-2241.
[15] K.K. Pandey, A note on the influence of extractives on the photo-discoloration and photo-degradation of wood, Polymer degradation and stability, 87 (2005) 375-379.
[16] M. Mattonai, A. Watanabe, A. Shiono, E. Ribechini, Degradation of wood by UV light: A study by EGA-MS and Py-GC/MS with on line irradiation system, Journal of Analytical and Applied Pyrolysis, 139 (2019) 224-232.
[17] M. Pánek, L. Reinprecht, Colour stability and surface defects of naturally aged wood treated with transparent paints for exterior constructions, Wood Res, 59 (2014) 421-430.
[18] P. Ahola, Adhesion between paints and wooden substrates: effects of pre-treatments and weathering of wood, Materials and Structures, 28 (1995) 350-356.
[19] S.L. Bardage, J. Bjurman, Adhesion of waterborne paints to wood, Journal of Coatings Technology, 70 (1998) 39-47.
[20] M. Nejad, P. Cooper, Exterior wood coatings, Wood in Civil Engineering, (2017) 111-129.

[21] M. de Meijer, Review on the durability of exterior wood coatings with reduced VOC-content, Progress in Organic Coatings, 43 (2001) 217-225.
[22] F. Zareanshahraki, V. Mannari, Formulation and optimization of radiation-curable nonisocyanate polyurethane wood coatings by mixture experimental design, Journal of Coatings Technology and Research, 18 (2021) 695-715.
[23] E. Scrinzi, S. Rossi, F. Deflorian, C. Zanella, Evaluation of aesthetic durability of waterborne polyurethane coatings applied on wood for interior applications, Progress in Organic Coatings, 72 (2011) 81-87.
[24] X. Peng, Z. Zhang, B. Wang, W. Du, Research on the aging properties of exterior wood coatings, in: Proceedings of 2012 International Conference on Biobase Material Science and Engineering, 2012, pp. 121-126.
[25] R. Bansal, S. Nair, K.K. Pandey, UV resistant wood coating based on zinc oxide and cerium oxide dispersed linseed oil nano-emulsion, Materials Today Communications, 30 (2022) 103177.
[26] M. Nowaczyk-Organista, T. Oleszek, Weathering resistance of water-borne wood coatings modified with metal nano oxides, in: 27th International Conference on Wood Science and Technology, ICWST 2016: Implementation of Wood Science in Woodworking Sector - Proceedings, 2016, pp. 159-165.
[27] S. Veigel, G. Grüll, S. Pinkl, M. Obersriebnig, U. Müller, W. Gindl-Altmutter, Improving the mechanical resistance of waterborne wood coatings by adding cellulose nanofibres, Reactive and Functional Polymers, 85 (2014) 214-220.
[28] P. Hochmańska-Kaniewska, D. Janiszewska, T. Oleszek, Enhancement of the properties of acrylic wood coatings with the use of biopolymers, Progress in Organic Coatings, 162 (2022) 106522.
[29] K. Šimůnková, Š. Hýsek, L. Reinprecht, J. Šobotník, T. Lišková, M. Pánek, Lavender oil as eco-friendly alternative to protect wood against termites without negative effect on wood properties, Scientific Reports, 12 (2022) 1-10.
[30] S.M. Miri Tari, A. Tarmian, M. Azadfallah, Improving fungal decay resistance of solvent and waterborne polyurethane-coated wood by free and microencapsulated thyme essential oil, Journal of Coatings Technology and Research, (2022).
[31] M.C. Wiemann, Characteristics and availability of commercially important woods, in, 2010.
[32] M. Nikolic, J.M. Lawther, A.R. Sanadi, Use of nanofillers in wood coatings: a scientific review, Journal of Coatings Technology and Research, 12 (2015) 445-461.
[33] P.D. Evans, P.D. Thay, K.J. Schmalzl, Degradation of wood surfaces during natural weathering. Effects on lignin and cellulose and on the adhesion of acrylic latex primers, Wood Science and Technology, 30 (2004) 411-422.
[34] N. Auclair, B. Riedl, V. Blanchard, P. Blanchet, Improvement of Photoprotection of Wood Coatings by Using Inorganic Nanoparticles as Ultraviolet Absorbers, Forest Products Journal, 61 (2011) 20-27.
[35] N. Allen, M. Edge, A. Ortega, C. Liauw, J. Stratton, R. McIntyre, Behaviour of nanoparticle (ultrafine) titanium dioxide pigments and stabilisers on the photooxidative stability of water based acrylic and isocyanate based acrylic coatings, Polymer Degradation and Stability, 78 (2002) 467-478.
[36] N. Veronovski, D. Verhovaek, J. Godnjavec, The influence of surface-treated nano-TiO_2 (rutile) incorporation in water-based acrylic coatings on wood protection, Wood Science and Technology, 47 (2012) 317-328.
[37] C.M. Pacheco, B.A. Cecilia, G. Reyes, C. Oviedo, A. Fernández-Pérez, M. Elso, O.J. Rojas, Nanocomposite additive of SiO_2/TiO_2/nanocellulose on waterborne coating formulations for mechanical and aesthetic properties stability on wood, Materials Today Communications, 29 (2021).
[38] S. Saha, D. Kocaefe, C. Krause, T. Larouche, Effect of titania and zinc oxide particles on acrylic polyurethane coating performance, Progress in Organic Coatings, 70 (2011) 170-177.
[39] J. Salla, K. Pandey, K. Srinivasa, Improvement of UV resistance of wood surfaces by using ZnO nanoparticles, Polymer Degradation and Stability, 97 (2012) 592–596.
[40] M.M. Jalili, S. Moradian, H. Dastmalchian, A. Karbasi, Investigating the variations in properties of 2-pack polyurethane clear coat through separate incorporation of hydrophilic and hydrophobic nano-silica, Progress in Organic Coatings, 59 (2007) 81-87.
[41] S. Saha, D. Kocaefe, Y. Boluk, A. Pichette, Surface degradation of CeO2 stabilized acrylic polyurethane coated thermally treated jack pine during accelerated weathering, Applied surface science, 276 (2013) 86-94.

[42] J. Janesch, I. Czabany, C. Hansmann, A. Mautner, T. Rosenau, W. Gindl-Altmutter, Transparent layer-by-layer coatings based on biopolymers and CeO2 to protect wood from UV light, Progress in Organic Coatings, 138 (2020).
[43] N.G.N. Salleh, M.S. Alias, H. Gläsel, R. Mehnert, High performance radiation curable hybrid coatings, Radiation Physics and Chemistry, 84 (2013) 70-73.
[44] S. Zhang, M. Guo, Z. Chen, Q.H. Liu, X. Liu, Grafting photosensitive polyurethane onto colloidal silica for use in UV-curing polyurethane nanocomposites, Colloids and Surfaces A: Physicochemical and Engineering Aspects, 443 (2014) 525-534.
[45] A.M. Cheumani Yona, J. Žigon, A. Ngueteu Kamlo, M. Pavlič, S. Dahle, M. Petrič, Preparation, Surface Characterization, and Water Resistance of Silicate and Sol-Silicate Inorganic–Organic Hybrid Dispersion Coatings for Wood, Materials, 14 (2021) 3559.
[46] C. Sow, B. Riedl, P. Blanchet, UV-waterborne polyurethane-acrylate nanocomposite coatings containing alumina and silica nanoparticles for wood: mechanical, optical, and thermal properties assessment, Journal of Coatings Technology and Research, 8 (2011) 211-221.
[47] J. Yang, H. Li, Z. Yi, M. Liao, Z. Qin, Stable superhydrophobic wood surface constracting by KH580 and nano-Al2O3 on polydopamine coating with two process methods, Colloids and Surfaces A: Physicochemical and Engineering Aspects, (2022) 128219.
[48] T.M. Pique, C.J. Perez, V.A. Alvarez, A. Vazquez, Water soluble nanocomposite films based on poly (vinyl alcohol) and chemically modified montmorillonites, Journal of Composite Materials, 48 (2014) 545-553.
[49] W.N. Nkeuwa, B. Riedl, V. Landry, Transparent UV-cured clay/UV-based nanocomposite coatings on wood substrates: surface roughness and effect of relative humidity on optical properties, Journal of Coatings Technology and Research, 14 (2017) 555-569.
[50] X. Xu, F. Liu, L. Jiang, J. Zhu, D. Haagenson, D.P. Wiesenborn, Cellulose nanocrystals vs. cellulose nanofibrils: a comparative study on their microstructures and effects as polymer reinforcing agents, ACS applied materials & interfaces, 5 (2013) 2999-3009.
[51] C.M. Pacheco, B.A. Cecilia, G. Reyes, C. Oviedo, A. Fernández-Pérez, M. Elso, O.J. Rojas, Nanocomposite additive of SiO2/TiO2/nanocellulose on waterborne coating formulations for mechanical and aesthetic properties stability on wood, Materials Today Communications, 29 (2021) 102990.
[52] H. Zou, S. Wu, J. Shen, Polymer/Silica Nanocomposites: Preparation, Characterization, Properties, and Applications, Chemical Reviews, 108 (2008) 3893-3957.
[53] B. Feng, S. Zhang, D. Wang, Y. Li, P. Zheng, L. Gao, D. Huo, L. Cheng, S. Wei, Study on antibacterial wood coatings with soybean protein isolate nano-silver hydrosol, Progress in Organic Coatings, (2022) 106766.
[54] J. Jusic, S. Tamantini, M. Romagnoli, V. Vinciguerra, E. Di Mattia, F. Zikeli, M. Cavalera, G. Scarascia Mugnozza, Improving sustainability in wood coating: testing lignin and cellulose nanocrystals as additives to commercial acrylic wood coatings for bio-building, iForest-Biogeosciences and Forestry, 14 (2021) 499.
[55] L. Yang, Y. Wu, F. Yang, W. Wang, The Effect of Antibacterial and Waterproof Coating Prepared From Hexadecyltrimethoxysilane and Nano-Titanium Dioxide on Wood Properties, Frontiers in Materials, 8 (2021) 261.
[56] S.M. Miri Tari, A. Tarmian, M. Azadfallah, Improving fungal decay resistance of solvent and waterborne polyurethane-coated wood by free and microencapsulated thyme essential oil, Journal of Coatings Technology and Research, (2022) 1-8.
[57] C.C. Tang, Y. Li, L.B. Kurnaz, J. Li, Development of eco-friendly antifungal coatings by curing natural seed oils on wood, Progress in Organic Coatings, 161 (2021) 106512.
[58] L. Rosu, F. Mustata, D. Rosu, C.-D. Varganici, I. Rosca, T. Rusu, Bio-based coatings from epoxy resins crosslinked with a rosin acid derivative for wood thermal and anti–fungal protection, Progress in Organic Coatings, 151 (2021) 106008.
[59] G. Kampf, D. Todt, S. Pfaender, E. Steinmann, Persistence of coronaviruses on inanimate surfaces and their inactivation with biocidal agents, Journal of hospital infection, 104 (2020) 246-251.
[60] H.A. Aboubakr, T.A. Sharafeldin, S.M. Goyal, Stability of SARS-CoV-2 and other coronaviruses in the environment and on common touch surfaces and the influence of climatic conditions: a review, Transboundary and emerging diseases, 68 (2021) 296-312.
[61] J. Otter, G. French, Bacterial contamination on touch surfaces in the public transport system and in public areas of a hospital in London, Letters in applied microbiology, 49 (2009) 803-805.

[62] N.K. Rai, A. Ashok, B.R. Akondi, Consequences of chemical impact of disinfectants: safe preventive measures against COVID-19, Critical reviews in toxicology, 50 (2020) 513-520.
[63] C. Gokce, C. Gurcan, O. Besbinar, M.A. Unal, A. Yilmazer, Emerging 2D materials for antimicrobial applications in the pre-and post-pandemic era, Nanoscale, (2021).
[64] W. Liu, R. Wang, V. Vedarethinam, L. Huang, K. Qian, Advanced materials for precise detection and antibiotic-free inhibition of bacteria, Materials Today Advances, 13 (2022) 100204.
[65] W. Li, E.S. Thian, M. Wang, Z. Wang, L. Ren, Surface design for antibacterial materials: from fundamentals to advanced strategies, Advanced Science, 8 (2021) 2100368.
[66] X. Yang, J. Hou, Y. Tian, J. Zhao, Q. Sun, S. Zhou, Antibacterial surfaces: Strategies and applications, Science China Technological Sciences, (2022) 1-11.
[67] V. Kotradyova, E. Vavrinsky, B. Kalinakova, D. Petro, K. Jansakova, M. Boles, H. Svobodova, Wood and its impact on humans and environment quality in health care facilities, International journal of environmental research and public health, 16 (2019) 3496.
[68] H. Xu, J. Li, M. Li, J. Wu, A Statistics-Based Study on Wood Presentation of Modern Wood Building Facades, in: MATEC Web of Conferences, EDP Sciences, 2019, pp. 01016.
[69] X. Duan, S. Liu, E. Huang, X. Shen, Z. Wang, S. Li, C. Jin, Superhydrophobic and antibacterial wood enabled by polydopamine-assisted decoration of copper nanoparticles, Colloids and Surfaces A: Physicochemical and Engineering Aspects, 602 (2020) 125145.
[70] L. Cheng, S. Ren, X. Lu, Application of eco-friendly waterborne polyurethane composite coating incorporated with nano cellulose crystalline and silver nano particles on wood antibacterial board, Polymers, 12 (2020) 407.
[71] L. Qian, L. Long, J.F. Xu, Surface modification of nano-titanium and its effect on the antibacterial property of waterborne wood coating, in: Key Engineering Materials, Trans Tech Publ, 2014, pp. 88-93.
[72] A. Russell, W. Hugo, 7 antimicrobial activity and action of silver, Progress in medicinal chemistry, 31 (1994) 351-370.
[73] K. Vithiya, R. Kumar, S. Sen, Antimicrobial activity of biosynthesized silver oxide nanoparticles, J. Pure Appl. Microbiol, 4 (2014) 3263-3268.
[74] M. Calovi, B. Furlan, V. Coroneo, O. Massidda, S. Rossi, Facile Route to Effective Antimicrobial Aluminum Oxide Layer Realized by Co-Deposition with Silver Nitrate, Coatings, 12 (2022) 28.
[75] I.X. Yin, J. Zhang, I.S. Zhao, M.L. Mei, Q. Li, C.H. Chu, The antibacterial mechanism of silver nanoparticles and its application in dentistry, International journal of nanomedicine, 15 (2020) 2555.
[76] G.V. Vimbela, S.M. Ngo, C. Fraze, L. Yang, D.A. Stout, Antibacterial properties and toxicity from metallic nanomaterials, International journal of nanomedicine, 12 (2017) 3941.
[77] T. Künniger, M. Heeb, M. Arnold, Antimicrobial efficacy of silver nanoparticles in transparent wood coatings, European Journal of Wood and Wood Products, 72 (2014) 285-288.
[78] A. Can, S. Palanti, H. Sivrikaya, B. Hazer, F. Stefanı, Physical, biological and chemical characterisation of wood treated with silver nanoparticles, Cellulose, 26 (2019) 5075-5084.
[79] L. Gao, Y. Lu, J. Li, Q. Sun, Superhydrophobic conductive wood with oil repellency obtained by coating with silver nanoparticles modified by fluoroalkyl silane, Holzforschung, 70 (2016) 63-68.
[80] X. Yan, P. Pan, Preparation of silver antibacterial agents with different forms and their effects on the properties of water-based primer on Tilia europaea surface, Coatings, 11 (2021) 1066.
[81] R. Moya, A. Rodriguez-Zuñiga, A. Berrocal, J. Vega-Baudrit, Effect of silver nanoparticles synthesized with NPsAg-ethylene glycol (C2H6O2) on brown decay and white decay fungi of nine tropical woods, Journal of Nanoscience and Nanotechnology, 17 (2017) 5233-5240.
[82] B. Goodell, Y. Qian, J. Jellison, Fungal decay of wood: soft rot—brown rot—white rot, in, ACS Publications, 2008.
[83] A. Cogulet, P. Blanchet, V. Landry, The multifactorial aspect of wood weathering: a review based on a holistic approach of wood degradation protected by clear coating, BioResources, 13 (2017) 2116 - 2138.
[84] S. Bardage, G. Daniel, The ability of fungi to penetrate micropores: implications for wood surface coatings, Material und Organismen (Germany), (1997).
[85] L. Rosu, C.D. Varganici, F. Mustata, D. Rosu, I. Rosca, T. Rusu, Epoxy coatings based on modified vegetable oils for wood surface protection against fungal degradation, ACS Applied Materials & Interfaces, 12 (2020) 14443-14458.

[86] M. Nejad, R. Shafaghi, L. Pershin, J. Mostaghimi, P. Cooper, Thermal spray coating: A new way of protecting wood, BioResources, 12 (2017) 143-156.
[87] R. Stirling, A. Uzunovic, P.I. Morris, Control of black stain fungi with biocides in semitransparent wood coatings, Forest products journal, 61 (2011) 359-364.
[88] N. Bellotti, R. Romagnoli, C. Quintero, C. Domínguez-Wong, F. Ruiz, C. Deyá, Nanoparticles as antifungal additives for indoor water borne paints, Progress in Organic Coatings, 86 (2015) 33-40.
[89] F. Ohashi, A. Shibahara, Antibacterial and antifungal properties of clear coating film containing silver–cytokinin complex as a filler, Journal of Coatings Technology and Research, 17 (2020) 1619-1623.
[90] R. Arreche, N. Bellotti, C. Deyá, P. Vázquez, Assessment of waterborne coatings formulated with sol-gel/Ag related to fungal growth resistance, Progress in Organic Coatings, 108 (2017) 36-43.
[91] A. Kumar, P.K. Vemula, P.M. Ajayan, G. John, Silver-nanoparticle-embedded antimicrobial paints based on vegetable oil, Nature materials, 7 (2008) 236-241.
[92] C. Gaylarde, L. Morton, K. Loh, M. Shirakawa, Biodeterioration of external architectural paint films–A review, International Biodeterioration & Biodegradation, 65 (2011) 1189-1198.
[93] BS ISO 22196: 2011 - Measurement of Antibacterial Activity on Plastics and Other Non-Porous Surfaces, BSI British Standards, (2011) 1-15.
[94] V. Kamperidou, The biological durability of thermally-and chemically-modified black pine and poplar wood against basidiomycetes and mold action, Forests, 10 (2019) 1111.
[95] Y. Gao, L. Zhao, J. Jiang, Z. Li, J. Lyu, Water Absorption Properties in Transverse Direction of Heat-Treated Chinese Fir Wood Determined Using TD-NMR, Forests, 12 (2021) 1545.
[96] C. Brischke, G. Alfredsen, Wood-water relationships and their role for wood susceptibility to fungal decay, Applied Microbiology and Biotechnology, 104 (2020) 3781-3795.
[97] G.S. Bobadilha, C.E. Stokes, G. Kirker, S.A. Ahmed, K.M. Ohno, D.J.V. Lopes, Effect of exterior wood coatings on the durability of cross-laminated timber against mold and decay fungi, BioResouces. 15 (4): 8420-8433., 15 (2020) 8420-8433.
[98] ASTM D3359-17 - Standard Test Methods for Rating Adhesion by Tape Test, West Conshohocken (PA): ASTM International, (2017) 1-10.
[99] S. Rossi, M. Fedel, S. Petrolli, F. Deflorian, Accelerated weathering and chemical resistance of polyurethane powder coatings, Journal of Coatings Technology and Research, 13 (2016) 427-437.
[100] X. Yang, C. Vang, D. Tallman, G. Bierwagen, S. Croll, S. Rohlik, Weathering degradation of a polyurethane coating, Polymer degradation and stability, 74 (2001) 341-351.
[101] Y. Zhang, J. Maxted, A. Barber, C. Lowe, R. Smith, The durability of clear polyurethane coil coatings studied by FTIR peak fitting, Polymer degradation and stability, 98 (2013) 527-534.
[102] A.M. Rabea, M. Mohseni, S. Mirabedini, M.H. Tabatabaei, Surface analysis and anti-graffiti behavior of a weathered polyurethane-based coating embedded with hydrophobic nano silica, Applied surface science, 258 (2012) 4391-4396.
[103] H. Wang, Y. Wang, D. Liu, Z. Sun, H. Wang, Effects of additives on weather-resistance properties of polyurethane films exposed to ultraviolet radiation and ozone atmosphere, Journal of Nanomaterials, 2014 (2014).
[104] A.M. Mittelman, J.D. Fortner, K.D. Pennell, Effects of ultraviolet light on silver nanoparticle mobility and dissolution, Environmental Science: Nano, 2 (2015) 683-691.
[105] N. Odzak, D. Kistler, L. Sigg, Influence of daylight on the fate of silver and zinc oxide nanoparticles in natural aquatic environments, Environmental Pollution, 226 (2017) 1-11.
[106] C.-C. Lin, D.-X. Lin, S.-H. Lin, Degradation problem in silver nanowire transparent electrodes caused by ultraviolet exposure, Nanotechnology, 31 (2020) 215705.
[107] ASTM G154:16 - Standard practice for operating fluorescent ultraviolet (UV) lamp apparatus for exposure of nonmetallic materials, West Conshohocken (PA): ASTM International, (2016).
[108] A. Cogulet, P. Blanchet, V. Landry, Wood degradation under UV irradiation: A lignin characterization, Journal of Photochemistry and Photobiology B: Biology, 158 (2016) 184-191.
[109] D. Cirule, E. Kuka, M. Kevers, I. Andersone, B. Andersons, Photodegradation of Unmodified and Thermally Modified Wood Due to Indoor Lighting, Forests, 12 (2021) 1060.
[110] M. Martí, B. Frígols, A. Serrano-Aroca, Antimicrobial characterization of advanced materials for bioengineering applications, JoVE (Journal of Visualized Experiments), (2018) e57710.

[111] E.C.f. Standardization, Durability of Wood and Wood-based Products: Wood-based Panels-Method of Test for Determining the Resistance Against Wood-destroying Basidiomycetes, European Committee for Standardization, 2002.
[112] M. Calovi, S. Rossi, Durability of Acrylic Cataphoretic Coatings Additivated with Colloidal Silver, Coatings, 12 (2022) 486.
[113] D. Fengel, G. Wegener, Wood: chemistry, ultrastructure, reactions, Walter de Gruyter, 2011.
[114] A. Ghavidel, M. Bak, T. Hofmann, V. Vasilache, I. Sandu, Evaluation of some wood-water relations and chemometric characteristics of recent oak and archaeological oak wood (Quercus Robur) with archaeometric value, Journal of Cultural Heritage, 51 (2021) 21-28.
[115] H. Bian, G. Li, L. Jiao, Z. Yu, H. Dai, Enzyme-assisted mechanical fibrillation of bleached spruce kraft pulp for producing well-dispersed and uniform-sized cellulose nanofibrils, Bioresources, 11 (2016) 10483-10496.
[116] R.B. Lima, R. Raza, H. Qin, J. Li, M.E. Lindström, B. Zhu, Direct lignin fuel cell for power generation, RSC advances, 3 (2013) 5083-5089.
[117] Y. Gu, H. Bian, L. Wei, R. Wang, Enhancement of hydrotropic fractionation of poplar wood using autohydrolysis and disk refining pretreatment: morphology and overall chemical characterization, Polymers, 11 (2019) 685.
[118] A. Ghavidel, R. Hosseinpourpia, J. Gelbrich, M. Bak, I. Sandu, Microstructural and chemical characteristics of archaeological white elm (Ulmus laevis P.) and poplar (Populus spp.), Applied Sciences, 11 (2021) 10271.
[119] H.-T. Lee, L.-H. Lin, Waterborne polyurethane/clay nanocomposites: novel effects of the clay and its interlayer ions on the morphology and physical and electrical properties, Macromolecules, 39 (2006) 6133-6141.
[120] ASTM E308-18 - Standard Practice for Computing the Colors of Objectives by Using the CIE System, West Conshohocken (PA): ASTM International, (2018).
[121] M. Hasani, M. Mahdavian, H. Yari, B. Ramezanzadeh, Versatile protection of exterior coatings by the aid of graphene oxide nano-sheets; comparison with conventional UV absorbers, Progress in Organic Coatings, 116 (2018) 90-101.
[122] G. Yi, S.N. Riduan, Y. Yuan, Y. Zhang, Microbicide surface nano-structures, Critical reviews in biotechnology, 39 (2019) 964-979.